Diabetes Advances Cardiomyocyte Senescence through miR-103a-3p/ Rnd3/STAT3 Signaling

Linxu Wu[1,*], Xinglin Zhu[1,*], Cai Luo[1,*], Yan Chen[1,*], Yin Liu[1], Yangyang Zhao[1], Shanshan Pan[1], Kaijia Shi[1], Jingci Xing[2], Xuebin Lin[1,3], Jianmin Qiu[1], Shuya Zhang[1], Jinxuan Chai[1], Zhihua Shen[2,✉], Wei Jie[1,✉], Junli Guo[1,✉]

[1] Hainan Provincial Key Laboratory of Tropical Cardiovascular Disease Research, the First Affiliated Hospital, Hainan Medical University, Haikou 570102, China.

[2]Department of Pathology and Pathophysiology, School of Basic Medicine Sciences, Guangdong Medical University, Zhanjiang 524023, China.

[3]Department of Medicine, Brigham and Women's Hospital of Harvard Medical School, Boston, MA, USA

*These authors contributed equally to this work.

✉Corresponding authors:

Prof. Zhihua Shen, Department of Pathology and Pathophysiology, School of Basic Medicine Sciences, Guangdong Medical University, Zhanjiang 524023, China. Tel +86-759-2388587, Email shenzh@gdmu.edu.cn

Prof. Wei Jie，Hainan Provincial Key Laboratory of Tropical Cardiovascular Disease Research, the First Affiliated Hospital, Hainan Medical University, Haikou 570102, China. Tel +86-898-66968217, Email wei_jie@hainmc.edu.cn;

Prof. Junli Guo，Hainan Provincial Key Laboratory of Tropical Cardiovascular Disease Research, the First Affiliated Hospital, Hainan Medical University, Haikou 570102, China. Tel +86-898-66968217, Email guojl@hainmc.edu.cn;

Abstract

Rnd3, a small Rho-GTPase, is involved in various cardiovascular diseases, but its role in diabetes-induced cardiomyocyte senescence is unclear. This study aims to investigate the role of Rnd3 in cardiomyocyte senescence in diabetes cardiomyopathy (DCM). *Rnd3* mRNA levels were reduced in peripheral blood mononuclear cells in diabetic patients, which was negatively correlated to patients age but positively correlated to cardiac function. Older mice exhibited compromised cardiac function, increased SA-β-gal-positive cells, and Senescence-associated secretory phenotype (SASP) marker levels versus younger mice. H9C2 and AC16 cardiomyocytes were exposed to high glucose ([HG] =35 mmol/L D-glucose), and an inhibited Rnd3 expression but enhanced cellular senescence were detected. *Rnd3* expression in H9C2 cells was disrupted using CRISPR/Cas9 technology, and a greater cellular senescence was observed in HG-insulted cardiomyocytes than that in normal glucose ([NG] =5.5 mmol/L D-glucose) control. MicroRNA sequencing was conducted on AC16 cells to identify differentially expressed microRNAs regulated by HG, and miR-103a-3p was identified as a key HG-regulated microRNA that binds to *Rnd3* 3′UTR. AAV9 carrying miR-103a-3p sponges and *Rnd3*-overexpressing plasmids mitigated cellular senescence in diabetic rats. Interestingly, miR-103a-3p levels positively correlated with blood glucose concentrations. HG stimulation amplified phosphorylated STAT3(Tyr705) in H9C2 cells, which was intensified by *Rnd3* knockout. Rnd3 binds with STAT3 in cytoplasm and promote proteasome-induced ubiquitination of STAT3. S3I-201 mitigated HG-activated STAT3 and cardiomyocyte senescence. Taken together, diabetes causes

cardiomyocyte senescence through miR-103a-3p/Rnd3/STAT3 signaling, suggesting a potential treatment strategy for DCM.

Keywords Diabetes cardiomyopathy, Rnd3, cardiomyocyte, cellular senescence, miR-103a-3p, STAT3

The medical and social demographic issues arising from global population aging are becoming increasingly prominent.[1] According to the World Health Organization, the global population at 65 years and older is projected to rise from 10% in 2022 to 16% in 2050.[2] This growth is occurring at an unprecedented rate and is expected to accelerate in the coming decades, especially in developing countries. Along with aging, the incidence of diabetes and other chronic diseases is also increasing. In 2021, approximately 537 million adults worldwide had diabetes, and the total number of people with diabetes is expected to increase to 783 million by 2045.[3] Diabetes alone caused 6.7 million deaths in 2021. Studies have shown a strong correlation between diabetes and aging, particularly in the population older than 65 years, where the prevalence of diabetes is as high as 25%–30%.[4] Unfortunately, aging and diabetes are considered independent risk factors for cardiovascular disease.[5,6] Furthermore, diabetes can exacerbate cellular aging, known as pathological senescence. Diabetes exacerbates age-related heart damage through mechanisms, such as fibrosis, NAD^+ metabolism abnormalities, oxidative stress, and autophagic inhibition.[7-11] Therefore, reducing cardiac cell senescence exacerbated by diabetes is important in preventing

cardiovascular events.

Aging cardiomyocytes exhibit contraction and metabolic dysfunction, and can secrete factors associated with the senescence-associated secretory phenotype (SASP), leading to remodeling of the local cardiac microenvironment.[11-12] Although various mechanisms can induce cardiomyocyte senescence, metabolic stressors, represented by diabetes, can induce the disease phenotype of cardiomyocytes.[12] Unlike the senescence of other cells, cardiomyocytes, as terminally differentiated cells, cannot simply be determined as experiencing senescence from cell cycle arrest. The aging of cardiomyocytes shows several features,[13-15] which was mainly manifested as DNA damage, SASP expression, systolic dysfunction, endoplasmic reticulum stress, cell hypertrophy and mitochondrial dysfunction. Although diabetes has been shown to be an important factor in promoting cardiomyocyte aging, senescent mechanisms and targets in the heart, especially under the diabetic condition, remain unclear.

Rnd3, also known as Rho family GTPase 3, is one of the atypical members of the Rho GTPase superfamily. Rnd3 is an endogenous inhibitor of Rho-associated kinase (ROCK) and plays an important role in cytoskeleton formation, cell proliferation, migration, and differentiation, the cell cycle, and apoptosis.[16,17] Rnd3 is involved in pathophysiological processes, such as brain edema caused by ependymal cell proliferation, cardiomyocyte apoptosis induced by stress overload, chronic heart failure, post-heart failure angiogenesis, arrhythmia, and post-infarction inflammation.[18-22] A recent report suggested that cardiac fibroblast-specific Rnd3 activation plays an important protective role in the pathogenesis of diabetic cardiomyopathy (DCM).[23]

These reports highlight the potential targeted value of Rnd3 in the treatment of cardiovascular disease.

This study mainly aimed to investigate the mechanistic role of Rnd3 in cardiomyocyte senescence under the diabetic condition. Our results show a novel role of dysregulation of Rnd3 in diabetes-induced cardiomyocyte senescence and suggest an alternative treatment strategy for DCM.

METHODS

For expanded methods, please see the Supplemental Material.

RESULTS

Rnd3 Expression in Human Tissue

To clarify the relationship between *Rnd3* and diabetes, we first searched the Gene Expression Omnibus (GEO) database for T2DM data. We found that *Rnd3* mRNA expression levels in peripheral blood mononuclear cells (GSE23561, GSE95849) and coronary tissue (GSE13760) in the T2DM population were significantly lower than those in the non-diabetic control groups (Fig. 1a). Then, used our cohort, we found that *Rnd3* mRNA expression in peripheral blood mononuclear cells of T2DM patients was significantly lower compared with that in controls (Fig. 1b, Table S1). Correlation analysis showed that *Rnd3* mRNA expression was significantly negatively correlated with age ($r=-0.546$, $P=0.001$), FBG (fasting blood glucose, $r=-0.368$, $P=0.0497$), cardiac troponin I (cTnI) ($r=-0.4666$, $P=0.0062$), myoglobin ($r=-0.6429$, $P<0.0001$),

NT-proBNP(r=−0.4087, *P*=0.0224), but positively correlated with EF% (r=0.5628, *P*=0.0007) and E/A ratio (r=0.4305, *P*=0.0357) (Fig. 1c). These results suggest that T2DM has an inhibitory effect on *Rnd3*, and that *Rnd3* mRNA expression is related to aging and myocardial injury.

Rnd3 **Expression and Cardiac Function in Aged Mice**

By comparing gene expression in heart tissue and cardiac function in juvenile and aged C56BL6/J mice (Fig. 2a), we found that the values of EF% and FS% in 60-week-old aged mice were significantly lower than those in young 7-week-old mice, but this did not reach the condition of heart failure (Fig. 2b). There were no obvious Senescence-associated β-galactosidase (SA-β-gal)-positive cells in the heart tissue of 7-week-old mice, while the number of SA-β-gal positive cells in the heart tissue of 60-week-old mice was significantly increased (Fig. 2c). Western blotting showed that Rnd3 protein levels were decreased in the aged mice, accompanied by an increase in cellular senescence markers, such as p53, p16, Monocyte chemoattractant protein-1 (MCP1), interleukin (IL)-6, IL1-α, and Growth differentiation factor 15 (GDF15) (Fig. 2d-e).

Diabetes Inhibits *Rnd3* Expression in Heart Tissue and Induces Cardiomyocyte Senescence

In streptozotocin (STZ)-induced Type 1 diabetes mellitus (T1DM) rats and spontaneous Type 2 diabetes mellitus (T2DM) mice (Fig. 3a), Rnd3 expression in heart tissue was significantly lower than that in controls (Fig. 3b). Considering that cardiomyocytes

highly expressed *Rnd3* in normal heart tissues (Fig. S1), we therefore consequently explore the role of diabetes on Rnd3 expression in cardiomyocytes. *In vitro* experiments also showed that high glucose (HG, 35 mmol/l D-glucose) stimulation effectively inhibited Rnd3 expression in cardiomyocytes (Fig. 3c), and this inhibition effect was glucose-dependent (Fig. S2). To further clarify the role of Rnd3 downregulation in cardiomyocyte senescence, we used CRISPR/Cas9 technology to construct H9C2 cells with *Rnd3* gene knockout (Fig. 3d). I*n vitro* HG stimulation significantly induced SA-β-gal-positive staining in H9C2 cells, and *Rnd3* gene knockout further amplified this effect (Fig. 3e). Additionally, DNA damage was aggravated (Fig. 3f) and the expression of SASP-related factors was upregulated (Fig. 3g, h).

Subsequently, we constructed the T2DM rat model with cardiomyocyte-specific *Rnd3* gene knockout (KO) and overexpression (Fig. 4a. The characteristics of these rats are shown in Fig. S3, Table S2). Echocardiography showed that T2DM adversely affected ejection fraction, fractional shortening and the E/A ratio in the heart, and *Rnd3* KO further aggravated this damage. Restoring *Rnd3* expression delayed the damage of T2DM to heart function (Fig. 4b, c). Western blotting showed that *Rnd3* KO promoted in cellular senescence markers levels induced by T2DM in heart tissue, while overexpressing *Rnd3* reduced the production of cellular senescence markers in heart tissue (Fig. 4d, e). γH2AX and SA-β-gal staining showed that *Rnd3* KO promoted the accumulation of γH2AX- and SA-β-gal-positive cells in the heart tissue of diabetic rats, while *Rnd3* overexpression reversed this effect (Fig. 4f-i).

HG Stimulation Upregulates miR-103a-3p to Inhibit *Rnd3* Expression in Cardiomyocytes

We hypothesized that microRNA (miRNA) plays a major role in the HG-induced inhibition of Rnd3 expression. To test this hypothesis, we performed miRNA sequencing on AC16 cells cultured in NG (5.5 mmol/L D-glucose) and HG (35 mmol/L D-glucose) to identify miRNAs that are regulated by glucose and target *Rnd3*. We found that, after 48 hours of treatment with HG, there were 43 differentially expressed miRNAs (23 upregulated and 20 downregulated) in AC16 cells compared with NG treatment (Table S3). Considering that most miRNAs inhibit the expression of their target genes. Therefore, we focused on miRNAs that were upregulated by HG stimulation. We observed that miR-103a-3p was closely related to T2DM and cellular senescence (Fig. 5a). Further experiments showed that miR-103a-3p expression was increased in cardiomyocytes stimulated by HG *in vitro* (Fig. 5b). By comparing the base sequences of miR-103a-3p and *Rnd3*, we found that miR-103a-3p was highly conserved between humans and rats. There was one binding site at position 1379 on the 3′UTR of the human *Rnd3* gene, and two binding sites at positions 579 and 716 on the 3′UTR of the rat *Rnd3* gene (Fig. 5c). The results of the luciferase reporter gene experiment supported the inhibitory effect of miR-103a-3p on the 3′UTR promoter of the *Rnd3* gene (Fig. 5d). We also examined miR-103a-3p concentrations in plasma of a clinical cohort including 24 cases of T2DM and 17 controls (see Table S4 for the clinical data of individuals). Interestingly, miR-103a-3p concentrations were significantly higher in the clinical T2DM population than in the non-diabetic controls (Fig. 5e). Additionally,

miR-103a-3p concentrations were positively correlated with FBG concentrations (r=0.408, *P*=0.0041) and the triglyceride and glucose index (r=0.441, *P*=0.002) (Fig. 5f).

Downregulating miR-103a-3p *in vitro* Restores Rnd3 Expression and Alleviates HG-Induced Cardiomyocyte Aging

To investigate the therapeutic value of targeting miR-103a-3p for diabetes-induced cardiomyocyte aging, we designed an inhibitor molecule for miR-103a-3p and applied it to H9C2 cardiomyocytes stimulated with HG (35 mmol/L D-glucose). After the administration of the miR-103a-3p inhibitor, *Rnd3* expression levels in cardiomyocytes were significantly increased, accompanied by downregulation of cellular senescence related genes expression (Fig. 6a, b, Fig. S4). SA-β-gal and γH2AX staining suggested that the miR-103a-3p inhibitor effectively alleviated diabetes-mediated cardiomyocyte senescence and DNA damage (Fig. 6c, d). These findings laid the foundation for the following *in vivo* experiments.

Cardiac Overexpression of miR-103a-3p Sponges Restores *Rnd3* Expression and Improves Heart Function in Diabetic Rats

To further evaluate the therapeutic effect of antagonizing miR-103a-3p on diabetes-induced myocardial aging, we constructed a T2DM rat model by a high-fat diet supplemented with intraperitoneal injection of STZ. One week later, AAV9-overexpressing miR103a-3p_sponges and negative control AAV9 were infused into the

rat tail vein (Fig. 7a. The characteristics of these rats are shown in Table S5). We found that the EF%, FS% and E/A peak values in diabetic rats in the overexpressed miR-103a-3p_sponge group were significantly better than those in diabetic rats injected with the control virus (Fig. 7b, c). Western blotting showed that overexpression of miR103a-3p_sponges effectively relieved the inhibitory effect of T2DM on Rnd3 protein levels in cardiac tissue, and also reduced SASP protein levels (Fig. 7d, e), consistent with the results of PCR (Fig. S5). The positive rates of SA-β-gal and γH2AX staining in myocardial cells in T2DM rats were significantly higher than those in controls. Additionally, the positive rates of SA-β-gal and γH2AX staining in T2DM rats infused with AAV9-miR-103a-3p_sponges were significantly lower than those in controls (Fig. 7e-h). These findings suggest that inhibiting miR-103a-3p and thereby restoring *Rnd3* expression is an effective means of disrupting diabetes-induced myocardial aging.

Downregulation of Rnd3 Induces a Cellular Senescence Phenotype in Cardiomyocytes by Activating the STAT3 Pathway

Finally, we examined the potential mechanism by which HG-suppressed Rnd3 expression promotes cardiac aging. STAT3, which is a transcription factor related to inflammation-associated SASP, may mediate this effect. T2DM rats showed higher phosphorylated (p)-STAT3(Tyr705) levels than control wild type rats, but Rnd3 overexpression was inhibited, while *Rnd3* knockout enhanced p-STAT3 (Tyr705) levels in the T2DM rat heart (Fig. S6a). Furthermore, *in vitro* HG stimulation led to the upregulation of p-STAT3(Tyr705) in cardiomyocytes, and *Rnd3* knockout amplified the

level of p-STAT3 (Tyr705) stimulated by HG (Fig. S6b). While administering S3I-201, p-STAT3 (Tyr705) levels decreased, and the expression of all proteins related to SASP (GDF15, IL-1α, IL-6, and MCP1), except for p53 and Rnd3, was also reduced (Fig. 8a, Fig. S6c). We also confirmed that HG stimuli could profoundly activated p-STAT3 (Tyr705) in *Rnd3* KO cardiomyocytes (Fig. 8b). Mechanistically, *Rnd3* KO led to obviously attenuated p-STAT3(Tyr705) ubiquitination through proteasome (Fig. 8c). what's more, a binding between Rnd3 and total STAT3 in cardiomycytes was detected (Fig. 8d). Interestingly, S3I-201 attenuated HG stimuli-induced nuclei accumulation of p-STAT3(Tyr705) (Fig. 8e), as well as HG-induced SA-β-gal-positive cells mostly in *Rnd3* knockout cells (Fig. 8f). These findings suggest that the STAT3 signal is involved in cardiac cell aging induced by the downregulation of Rnd3 expression and is mediated by diabetic stimulation. Overall, the activation of the miR-103a-3p/Rnd3/STAT3 signal plays an important role in diabetes-induced cardiac cell aging, and also has the potential for targeted intervention (Fig. 8g).

DISCUSSION

Rnd3 has become the focus of attention from scholars worldwide for its association with cancer.[17] Our research group, in collaboration with Dr Chang, has been investigating the relationship between *Rnd3* and cardiovascular disease for more than a decade.[17,19,21,22] Other research groups have also suggested that *Rnd3* plays a crucial role in vascular and cardiac remodeling.[23,24] These findings suggest that *Rnd3* may have considerable therapeutic value in cardiovascular disease. This study further extends the

role of *Rnd3* in diabetes-induced cardiomyocyte aging. We found that downregulation of *Rnd3* expression exacerbated diabetes-induced cardiomyocyte senescence, possibly due to diabetes-induced elevation of miR-103a-3p, which directly inhibits *Rnd3*. This process then activated STAT3 signaling and promoted cardiomyocyte senescence. Interestingly, targeted inhibition of miR-103a-3p and overexpression of *Rnd3* helped in restoring *Rnd3* expression in DCM and reversed cardiomyocyte senescence. This study provides a potentially feasible strategy for the prevention and treatment of DCM aging.

Since the Framingham study first reported that diabetes can aggravate cardiovascular mortality,[25] the rapidly growing number of diabetes populations worldwide has led to attention being paid to the cardiovascular complications of diabetes. Our study first examined the relationship between *Rnd3* and diabetes using the GEO dataset, and we found downregulation of *Rnd3* mRNA levels in patients with diabetes. According to the International Diabetes Federation, the global population with diabetes was approximately 463 million in 2019 and is expected to increase to 578 million by 2030.[26] Cardiovascular events associated with diabetes have become major causes of death and disability in diabetes, making the prevention and treatment of diabetes a major global public health issue. These results based on the GEO public database provide a platform for further in-depth exploration of the relationship and regulatory mechanism between abnormal *Rnd3* expression and diabetes.

The long-term pathological state of diabetes, such as hyperglycemia, hyperlipidemia, insulin resistance, and oxidative stress, can accelerate cardiac cell aging and injury.[8,27,28] This process is different from the mechanism of cell aging caused

by a simple increase in age. In our cohort, we found that *Rnd3* mRNA levels were negatively correlated with the population's age (i.e., as age increased, *Rnd3* mRNA levels decreased), suggesting a relationship between *Rnd3* levels and aging. This result is consistent with the results of Rnd3 expression, heart function, and cellular senescence markers in the heart tissue of young and old mice. Further correlation analysis showed that *Rnd3* levels were also related to some factors of myocardial injury, such as cTnI, myoglubin, NT-proBNP and cardiac function markers like EF% and E/A ratio. These results further confirm our initial assumption. Therefore, we will verify our results through cell and animal experiments in subsequent research.

The approach based on single-cell RNA sequencing has recently received much attention, providing the possibility to analyze the composition of organ and cell changes under different states.[29] Using bioinformatics, we found that normal human heart tissue contained various cell types, and the *Rnd3* gene had the highest abundance of expression in certain subtype of cardiomyocytes. These findings suggest that *Rnd3* plays a crucial role in cardiac cells. On the basis of this finding, we constructed a rodent model of cardiac *Rnd3* overexpression and knockout, and obtained H9C2 cardiomyocytes with stable knockout of the *Rnd3* gene using CRISPR/Cas9 technology. The successful establishment of these animal and cell models laid a solid foundation for the implementation of this study.

On the basis of the finding that *Rnd3* expression was present in diabetic heart tissue and HG-treated cardiomyocytes, we constructed H9C2 cells with *Rnd3* gene knockout based on previous protocols.[30] Our study showed that *Rnd3* knockout cells stimulated

by HG were more likely to show cell cycle arrest and SASP. SASP is a key feature of cell aging, and related factors play a decisive regulatory role in processes, such as cellular senescence, inflammation, immune modulation, growth arrest, fibrosis, and tumorigenesis.[31] Therefore, the lack of *Rnd3* expression contributes to HG-induced cardiomyocyte senescence. Indeed, *Rnd3* gene knockout amplified the diabetes-induced myocardial damage. In contrast, overexpressing *Rnd3* in heart tissue through tail vein injection of AAV9 restored heart function and alleviated the SASP. Considering the clinically significant relevance of cellular senescence in the management of patients with cardiac diseases,[32] the current study suggests that targeting *Rnd3* to reverse myocardial cell aging could considerably enhance the treatment of DCM.

Upon finding that diabetes induced cardiomyocyte senescence by suppressing *Rnd3* expression, this study focused on the epigenetics of miRNA. The miRNAs are endogenous non-coding RNAs of approximately 22 nt in length, and they play a universal inhibitory role in gene silencing.[33] Ihe potential of miRNA as a therapeutic target for cardiovascular aging is gradually gaining attention.[34,35] We hypothesized that there are certain miRNAs that target the *Rnd3'*UTR and they are upregulated during diabetes. To test this hypothesis, we performed miRNA sequencing on AC16 cells cultured under different glucose concentrations to screen for differentially expressed miRNAs. We discovered numerous differentially expressed miRNAs in AC16 cardiomyocytes stimulated by HG. We searched for the conservation of differentially expressed miRNAs among species through the microRNA viewer website, and prioritized miR-103a-3p, which is fully conserved between humans and rats, for further

research. Bioinformatics analysis showed that the target genes of miR-103a-3p were involved in numerous pathological physiological processes, such as aging, cardiovascular disease, and endocrine disease. This miRNA plays a regulatory role in various biological processes, such as sugar, lipid, vitamin, and energy metabolism, tissue regeneration, signal transduction, and inflammatory responses. Using quantitative RT-PCR, we found that miR-103a-3p expression in human and rat cardiomyocytes was increased under glucose stimulation, suggesting that miR-103a-3p may be an appropriate target in diabetic damage. Subsequent *in vitro* experiments suggested that directly using an miR-103a-3p inhibitor restored *Rnd3* expression in H9C2 cells under HG conditions, and simultaneously reduced HG-induced cardiomyocyte senescence. Using *in vivo* experiments, our study further showed that overexpressing miR-103a-3p sponges delayed the damage in heart function caused by diabetes in rats, and inhibited the expression of cellular senescence related factors in rat heart tissue. Most importantly, we found that blood glucose concentration-related circulating miR-103a-3p levels were upregulated in the diabetes population compared with non-diabetes controls. Therefore, miR-103a-3p could be involved in diabetes-suppressed *Rnd3* expression. No gross complications were observed in rats administered miR-103a-3p sponges, and their survival rate was not different from that in the control group during the experimental period. However, the safety of AAV9-administered miR-103a-3p sponges in other tissues and organs still needs more comprehensive verification. There are more than 150 reports regarding miR-103a-3p in PubMed; among them, only one report focused on cardiomyocytes,[36] and one meta-

analysis suggested that miR-103a-3p could be a biomarker for T2DM.[37] Our current research expands the application of miR-103a-3p in DCM treatment.

Rnd3 reduces oxidative stress, cell proliferation, fibrosis, and the inflammatory response by inhibiting ROCK1, nuclear factor kappa-B, Notch, and transforming growth factor-β signals in various cells and tissues,[18,22,23,34] and these signals are also crucial for driving cardiac aging. Our previous study showed that *Rnd3* knockout activated the Jak/STAT pathway.[30] Activation of STAT3 signaling is pivotal for cell-to-cell communication in the heart.[38] This finding laid the foundation for our subsequent analysis of how Rnd3 downregulation mediates cardiomyocyte senescence. Reports have shown that p-STAT3 is upregulated with HG stimulation and promotes the expression of SASP-related inflammatory factors,[39,40] as found in this study. Most important, our current investigation for the first time revealed that Rnd3 could interacts with STAT3 in cardiomyocyes, and this binding provoked the ubiquitination of p-STAT3. These findings suggest that HG stimulation and *Rnd3* knockout upregulate p-STAT3 expression, with its mechanism was mostly related to ubiquitination mediated degradation pathway.

STAT3 activation plays protective or pathogenic roles under different pathophysiological conditions in the cardiovascular system. IL-6 is a key activator of STAT3. IL-6 mediates left ventricular hypertrophy and myocardial fibrosis by activating STAT3 signaling.[41,42] However, Granulocyte Colony Stimulating Factor prevents post-infarction ventricular remodeling by activating the JAK/STAT pathway.[43] Moreover, cardiac-specific knockout of STAT3 exacerbates subacute ventricular

remodeling in mice with myocardial infarction.[44] In the current study, we observed that the expression of SASP-related factors, such as IL-6, MCP1, and IL-1α, was increased with the knockout of *Rnd3*, along with upregulation of p-STAT3. These SASPs and the STAT3 pathway have a mutual regulatory effect. In particular, IL-6 and MCP1 can promote STAT3 phosphorylation, and STAT3 phosphorylation further increases the expression levels of IL-6 and MCP1.[41,45,46] To further clarify the upstream and downstream relationship between Rnd3, SASP, and STAT3, we used the highly selective STAT3 inhibitor S3I-201[47]. Interestingly, regardless of the group (wild type or *Rnd3* knockout), treating H9C2 cells with S3I-201 significantly inhibited the expression of SASP-related factors, such as IL-1α, IL-6, and MCP1, but not Rnd3, in parallel with the attenuation of SA-β-gal-positive cells. These findings suggest that the activation of STAT3 is a key pathway involved in diabetes-/HG-induced cardiomyocyte senescence through inhibiting *Rnd3*. A recent reported showed that blocking aged-related inflammatory responses is important in the treatment of aging and degeneration of the nervous system.[48] Our study showed that targeted intervention of miR-103a-3p/Rnd3/STAT3 signaling in diabetes blocked the expression of SASP-related inflammatory factors and thus reduced cardiomyocyte cell aging, which is consistent with the above-mentioned findings.

LIMITATIONS

There are some limitations to our study. First, the heart is composed of various cell types. Our study only focused on the effect of *Rnd3* expression defects under diabetes

on the aging of cardiomyocytes. Further research is required to investigate whether there are other mechanisms between various cells that affect cardiac aging. Second, abnormal *Rnd3* expression also involves other signaling pathways that affect myocardial aging, Therefore, using multiomics such as proteomics methods may reveal more signaling pathways affected by *Rnd3* dysregulation.

CONCLUSION

Diabetes induces cardiomyocyte senescence by upregulating miR-103a-3p, thereby suppressing *Rnd3* expression and subsequently activating STAT3 to elevate the transcription levels of SASP-related factors. Direct myocardial overexpression of *Rnd3* or genetic inhibition of miR-103a-3p or pharmacological inhibition of STAT3 can preserve cardiac function in diabetic rats and counteract cardiomyocyte cell senescence.

Affiliations

Hainan Provincial Key Laboratory for Tropical Cardiovascular Disease Research, the First Affiliated Hospital, Hainan Medical University, Haikou, China (L. Wu, C. Luo, X. Zhu, Y. Chen, Y. Liu, Y. Zhao, S. Pan, K, Shi, X. Ling, J. Qiu, S. Zhang, J. Chai, J. Guo, W. Jie), Department of Pathology and Pathophysiology, School of Basic Medicine Sciences, Guangdong Medical University, Zhanjiang, China (J. Xing, Z. Shen), and Department of Medicine, Brigham and Women's Hospital of Harvard Medical School, Boston, MA, USA (X. Ling).

.

Author Contributions

L. Wu, X. Zhu, C. Luo, Y. Chen, Y. Zhao, S. Pan, J. Xing, K. Shi, J. Qiu and S. Zhang performed the experiments and collected the data. Y. Liu and X. Ling collected the clinical samples and reviewed the data. L. Wu, XLZ, CL, and JXC prepared the materials. Z. Shen and X. Ling searched the literature and performed statistical analyses. Z. Shen, J. Guo, and W. Jie conceived and coordinated the study and drafted the manuscript. All of the authors read and approved the final manuscript.

Data availability statement

The original contributions presented in the study are included in the article/Supplemental Material. Further inquiries can be directed to the corresponding authors.

Sources of Funding

This work was supported by Hainan Key Research and Development Project (ZDYF2022SHFZ038, ZDYF2020122), the National Natural Science Foundation of China (82060053, 82260083, U220A20270), and the Cardiovascular Disease Research Science Innovation Group of Hainan Medical University. The funders had no role in the design of the study, collection, analysis or interpretation of the data, or writing the manuscript.

Disclosures

The authors have no conflicts of interest related to this work.

Ethics statement

All animal experiments conform to the ethical requirements for experimental animals of Hainan Medical University (Approval number: KYLL-2020-048). The use of human tissues was reviewed and approved by the Ethics Committee of the First Affiliated Hospital of Hainan Medical University (Approval number: 2023-KYL-096).

Supplemental Material

Supplemental Materials and Methods

Figures S1–S6

Tables S1–S5

References

1. Centers for Disease Control and Prevention (CDC). Trends in aging--United States and worldwide. *MMWR Morb Mortal Wkly Rep.* 2003;52(6):101-106.
2. United Nations, Department of Economic and Social Affairs, Population Division. World Population Prospects 2022: Ten Key Messages. 2022.
3. D Magliano DJ, Boyko EJ; IDF Diabetes Atlas 10th edition scientific committee. IDF DIABETES ATLAS [Internet]. 10th ed. Brussels: International Diabetes Federation; 2021.
4. American Diabetes Association. 11. Older Adults: Standards of Medical Care in Diabetes-2018. *Diabetes Care*. 2018;41(Suppl 1):S119-S125. doi:10.2337/dc18-S011
5. Dauriz M, Targher G, Laroche C, Temporelli PL, Ferrari R, Anker S, Coats A, Filippatos G, Crespo-Leiro M, Mebazaa A et al. Association Between Diabetes and 1-Year Adverse Clinical Outcomes in a Multinational Cohort of Ambulatory Patients With Chronic Heart Failure:

Results From the ESC-HFA Heart Failure Long-Term Registry. *Diabetes Care*. 2017;40(5):671-678. doi:10.2337/dc16-2016

6. North BJ, Sinclair DA. The intersection between aging and cardiovascular disease. *Circ Res.* 2012;110(8):1097-1108. doi:10.1161/CIRCRESAHA.111.246876

7. Jia G, Hill MA, Sowers JR. Diabetic Cardiomyopathy: An Update of Mechanisms Contributing to This Clinical Entity. *Circ Res*. 2018;122(4):624-638. doi:10.1161/CIRCRESAHA.117.311586

8. Jankauskas SS, Kansakar U, Varzideh F, Wilson S, Mone P, Lombardi A, Gambardella J, Santulli G. Heart failure in diabetes. *Metabolism*. 2021;125:154910. doi:10.1016/j.metabol.2021.154910

9. Abdellatif M, Sedej S, Kroemer G. NAD+ Metabolism in Cardiac Health, Aging, and Disease. *Circulation*.2021;144(22):1795-1817. doi:10.1161/CIRCULATIONAHA.121.056589

10. Dewanjee S, Vallamkondu J, Kalra RS, John A, Reddy PH, Kandimalla R. Autophagy in the diabetic heart: A potential pharmacotherapeutic target in diabetic cardiomyopathy. *Ageing Res Rev*. 2021;68:101338. doi:10.1016/j.arr.2021.101338

11. Chen MS, Lee RT, Garbern JC. Senescence mechanisms and targets in the heart. *Cardiovasc Res*. 2022;118(5):1173-1187. doi:10.1093/cvr/cvab161

12. Tang X, Li PH, Chen HZ. Cardiomyocyte Senescence and Cellular Communications Within Myocardial Microenvironments. *Front Endocrinol (Lausanne)*. 2020;11:280. doi:10.3389/fendo.2020.00280

13. Ribeiro ASF, Zerolo BE, López-Espuela F, Sánchez R, Fernandes VS. Cardiac System during the Aging Process. *Aging Dis*. 2023;14(4):1105-1122. doi:10.14336/AD.2023.0115

14. Abdellatif M, Rainer PP, Sedej S, Kroemer G. Hallmarks of cardiovascular ageing. *Nat Rev Cardiol.* 2023;20(11):754-777. doi:10.1038/s41569-023-00881-3

15. Cai Y, Song W, Li J, Jing Y, Liang C, Zhang L, Zhang X, Zhang W, Liu B, An Y et al. The landscape of aging. *Sci China Life Sci.* 2022;65(12):2354-2454. doi:10.1007/s11427-022-2161-3

16. Chardin P. Function and regulation of Rnd proteins. *Nat Rev Mol Cell Biol.* 2006;7(1):54-62. doi:10.1038/nrm1788

17. Jie W, Andrade KC, Lin X, Yang X, Yue X, Chang J. Pathophysiological Functions of Rnd3/RhoE. *Compr Physiol.* 2015;6(1):169-186. doi:10.1002/cphy.c150018

18. Lin X, Liu B, Yang X, Yue X, Diao L, Wang J, Chang J. Genetic deletion of Rnd3 results in aqueductal stenosis leading to hydrocephalus through up-regulation of Notch signaling. *Proc Natl Acad Sci U S A.* 2013;110(20):8236-8241. doi:10.1073/pnas.1219995110

19. Yue X, Yang X, Lin X, Yang T, Yi X, Dai Y, Guo J, Li T, Shi J, Wei L et al. Rnd3 haploinsufficient mice are predisposed to hemodynamic stress and develop apoptotic cardiomyopathy with heart failure. *Cell Death Dis.* 2014;5(6):e1284. doi:10.1038/cddis.2014.235

20. Yang X, Wang T, Lin X, Yue X, Wang Q, Wang G, Fu Q, Ai X, Chiang DY, Miyake CY et al. Genetic deletion of Rnd3/RhoE results in mouse heart calcium leakage through upregulation of protein kinase A signaling. *Circ Res.* 2015;116(1):e1-e10. doi:10.1161/CIRCRESAHA.116.304940

21. Yue X, Lin X, Yang T, Yang X, Yi X, Jiang X, Li X, Li T, Guo J, Dai Y et al. Rnd3/RhoE Modulates Hypoxia-Inducible Factor 1α/Vascular Endothelial Growth Factor Signaling by Stabilizing Hypoxia-Inducible Factor 1α and Regulates Responsive Cardiac Angiogenesis. *Hypertension.* 2016;67(3):597-605. doi:10.1161/HYPERTENSIONAHA.115.06412

22. Dai Y, Song J, Li W, Yang T, Yue X, Lin X, Yang X, Luo W, Guo J, Wang X et al. RhoE Fine-Tunes Inflammatory Response in Myocardial Infarction. *Circulation*.2019;139(9):1185-1198. doi:10.1161/CIRCULATIONAHA.118.033700

23. Zhang Y, Cao Y, Zheng R, Xiong Z, Zhu Z, Gao F, Man W, Duan Y, Lin J, Zhang X et al. Fibroblast-specific activation of Rnd3 protects against cardiac remodeling in diabetic cardiomyopathy via suppression of Notch and TGF-β signaling. *Theranostics.* 2022;12(17):7250-7266. doi:10.7150/thno.77043

24. Wu N, Zheng F, Li N, Han Y, Xiong XQ, Wang JJ, Chen Q, Li YH, Zhu GQ, Zhou YB. RND3 attenuates oxidative stress and vascular remodeling in spontaneously hypertensive rat via inhibiting ROCK1 signaling. *Redox Biol.* 2021, 48:102204. doi:10.1016/j.redox.2021.102204

25. Kannel WB, McGee DL. Diabetes and cardiovascular disease. The Framingham study. *JAMA.*

1979;241(19):2035-2038. doi:10.1001/jama.241.19.2035

26. Saeedi P, Petersohn I, Salpea P, Malanda B, Karuranga S, Unwin N, Colagiuri S, Guariguata L, Motala AA, Ogurtsova K et al. Global and regional diabetes prevalence estimates for 2019 and projections for 2030 and 2045: Results from the International Diabetes Federation Diabetes Atlas, 9(th) edition. *Diabetes Res Clin Pract*. 2019, 157:107843. doi:10.1016/j.diabres.2019.107843

27. Shakeri H, Lemmens K, Gevaert AB, De Meyer GRY, Segers VFM. Cellular senescence links aging and diabetes in cardiovascular disease. *Am J Physiol Heart Circ Physiol.* 2018, 315(3):H448-H462. doi:10.1152/ajpheart.00287.2018

28. Ritchie RH, Abel ED. Basic Mechanisms of Diabetic Heart Disease. *Circ Res.* 2020;126(11):1501-1525. doi:10.1161/CIRCRESAHA.120.315913

29. Jovic D, Liang X, Zeng H, Lin L, Xu F, Luo Y. Single-cell RNA sequencing technologies and applications: A brief overview. *Clin Transl Med*. 2022;12(3):e694. doi:10.1002/ctm2.694

30. Shao Z, Wang K, Zhang S, Yuan J, Liao X, Wu C, Zou Y, Ha Y, Shen Z, Guo J et al. Ingenuity pathway analysis of differentially expressed genes involved in signaling pathways and molecular networks in RhoE gene-edited cardiomyocytes. *Int J Mol Med. 2020*, 46(3):1225-1238. doi:10.3892/ijmm.2020.4661

31. Birch J, Gil J. Senescence and the SASP: many therapeutic avenues. *Genes Dev.* 2020;34(23-24):1565-1576. doi:10.1101/gad.343129.120

32. Mehdizadeh M, Aguilar M, Thorin E, Ferbeyre G, Nattel S. The role of cellular senescence in cardiac disease: basic biology and clinical relevance. *Nat Rev Cardiol*. 2022, 19(4):250-264. doi:10.1038/s41569-021-00624-2

33. Ha M, Kim VN. Regulation of microRNA biogenesis. *Nat Rev Mol Cell Biol*. 2014;15(8):509-524. doi:10.1038/nrm3838

34. Li H, Hastings MH, Rhee J, Trager LE, Roh JD, Rosenzweig A. Targeting Age-Related Pathways in Heart Failure. *Circ Res.* 2020;126(4):533-551. doi:10.1161/CIRCRESAHA.119.315889

35. Jusic A, Thomas PB, Wettinger SB, Dogan S, Farrugia R, Gaetano C, Tuna BG, Pinet F, Robinson EL, Tual-Chalot S et al. Noncoding RNAs in age-related cardiovascular diseases.

Ageing Res Rev. 2022, 77:101610. doi:10.1016/j.arr.2022.101610

36. Zhang C, Zhang C, Wang H, Qi Y, Kan Y, Ge Z. Effects of miR-103a-3p on the autophagy and apoptosis of cardiomyocytes by regulating Atg5. *Int J Mol Med*. 2019, 43(5):1951-1960. doi:10.3892/ijmm.2019.4128

37. Zhu H, Leung SW. MicroRNA biomarkers of type 2 diabetes: evidence synthesis from meta-analyses and pathway modelling. *Diabetologia*. 2023, 66(2):288-299. doi:10.1007/s00125-022-05809-z

38. Haghikia A, Ricke-Hoch M, Stapel B, Gorst I, Hilfiker-Kleiner D. STAT3, a key regulator of cell-to-cell communication in the heart. *Cardiovasc Res*. 2014, 102(2):281-289. doi:10.1093/cvr/cvu03

39. Sun HJ, Xiong SP, Cao X, Cao L, Zhu MY, Wu ZY, Bian JS. Polysulfide-mediated sulfhydration of SIRT1 prevents diabetic nephropathy by suppressing phosphorylation and acetylation of p65 NF-kappaB and STAT3. *Redox Biol*. 2021, 38:101813. doi:10.1016/j.redox.2020.101813

40. Yang WX, Liu Y, Zhang SM, Wang HF, Liu YF, Liu JL, Li XH, Zeng MR, Han YZ, Liu FY et al. Epac activation ameliorates tubulointerstitial inflammation in diabetic nephropathy. *Acta Pharmacol Sin*. 2022, 43(3):659-671. doi:10.1038/s41401-021-00689-2

41. Zhao L, Cheng G, Jin R, Afzal MR, Samanta A, Xuan YT, Girgis M, Elias HK, Zhu Y, Davani A et al. Deletion of Interleukin-6 Attenuates Pressure Overload-Induced Left Ventricular Hypertrophy and Dysfunction. *Circ Res*. 2016, 118(12):1918-1929. doi:10.1161/CIRCRESAHA.116.308688

42. Datta R, Bansal T, Rana S, Datta K, Datta Chaudhuri R, Chawla-Sarkar M, Sarkar S. Myocyte-Derived Hsp90 Modulates Collagen Upregulation via Biphasic Activation of STAT-3 in Fibroblasts during Cardiac Hypertrophy. *Mol Cell Biol*. 2017, 37(6). doi:10.1128/MCB.00611-16

43. Harada M, Qin Y, Takano H, Minamino T, Zou Y, Toko H, Ohtsuka M, Matsuura K, Sano M, Nishi J et al. G-CSF prevents cardiac remodeling after myocardial infarction by activating the Jak-Stat pathway in cardiomyocytes. *Nat Med*. 2005, 11(3):305-311. doi:10.1038/nm1199

44. Enomoto D, Obana M, Miyawaki A, Maeda M, Nakayama H, Fujio Y. Cardiac-specific ablation of the STAT3 gene in the subacute phase of myocardial infarction exacerbated cardiac

remodeling. *Am J Physiol Heart Circ Physiol*. 2015, 309(3):H471-480. doi:10.1152/ajpheart.00730.2014

45. Yasuda T, Koiwa M, Yonemura A, Miyake K, Kariya R, Kubota S, Yokomizo-Nakano T, Yasuda-Yoshihara N, Uchihara T, Itoyama R et al. Inflammation-driven senescence-associated secretory phenotype in cancer-associated fibroblasts enhances peritoneal dissemination. *Cell Rep*. 2021, 34(8):108779. doi:10.1016/j.celrep.2021.108779

46. Yan W, Tu B, Liu YY, Wang TY, Qiao H, Zhai ZJ, Li HW, Tang TT. Suppressive Effects of Plumbagin on Invasion and Migration of Breast Cancer Cells via the Inhibition of STAT3 Signaling and Down-regulation of Inflammatory Cytokine Expressions. *Bone Res*. 2013, 1(4):362-370. doi:10.4248/BR201304007

47. Siddiquee K, Zhang S, Guida WC, Blaskovich MA, Greedy B, Lawrence HR, Yip ML, Jove R, McLaughlin MM, Lawrence NJ et al. Selective chemical probe inhibitor of Stat3, identified through structure-based virtual screening, induces antitumor activity. *Proc Natl Acad Sci U S A*. 2007, 104(18):7391-7396. doi:10.1073/pnas.0609757104

48. Gulen MF, Samson N, Keller A, Schwabenland M, Liu C, Gluck S, Thacker VV, Favre L, Mangeat B, Kroese LJ et al. cGAS-STING drives ageing-related inflammation and neurodegeneration. *Nature*. 2023, 620(7973):374-380. doi:10.1038/s41586-023-06373-1

Figure legends

Figure 1. *Rnd3* expression in human tissue based on public databases and a clinical cohort. (**A**) Datasets in Gene Expression Omnibus (GEO) showed that *Rnd3* mRNA levels were enhanced in peripheral blood cells (GSE23561, GSE95849) and coronary artery media (GSE13760) in patients with diabetes compared with controls. Data were analyzed by the Mann–Whitney test; **P*<0.05, ***P*<0.01, *****P*<0.0001. (**B**) *Rnd3* mRNA levels in peripheral blood mononuclear cells of a clinical cohort Diabetic patients and non-diabetic patients. Data were analyzed by the Mann–Whitney test;

*P<0.05. (**C**) Spearman correlation analysis of *Rnd3* mRNA levels with fasting blood glucose (FBG), age, cardiac troponin I (cTnI), myoglobin, NT-proBNP, ejection fraction (EF%) and E/A ratio in a clinical cohort.

Figure 2. *Rnd3* expression and cardiac function in juvenile and aged mice. (**A**) Schematic diagram of the experimental procedure. (**B**) Ultrasound detection of cardiac function in young and older mice. Data were analyzed by the unpaired t test; **P<0.01. (**C**) SA-β-galactosidase staining using frozen sections of the mouse heart. Data were analyzed by the unpaired t test; **P<0.01. (**D**) Western blot detection of Rnd3 and cell cycle-related p53 and p16 protein levels, and the SASP-related proteins IL-1α, IL-6, and GDF15. β-actin served as an internal reference. (**E**) Quantitative analysis of Rnd3, p53, and p16 protein levels and the SASP-related genes IL-1α, IL6, and GDF15. Data were analyzed by the unpaired t test; **P<0.01, ***P<0.001.

Figure 3. Effects of diabetes/high glucose on *Rnd3* expression and cell senescence in cardiomyocytes. (**A**) Schematic diagram of the establishment of T1DM and T2DM models. (**B**) Western blot detection of Rnd3 protein levels in heart tissue of diabetic rats and mice. β-actin served as an internal reference. Data were analyzed by the unpaired t test; *P<0.05. (**C**) Western blot detection of Rnd3 protein levels in high glucose (HG) (35 mmol/L D-glucose)-treated cardiomyocytes. Data were analyzed by the unpaired t test; **P<0.01, ***P<0.001. (**D**) Establishment of *Rnd3* gene knockout H9C2 cardiomyocytes using CRISPR/Cas9 technology. Data were analyzed by the unpaired t

test; **P<0.01. (**E**) SA-β-galactosidase staining in normal glucose (NG)- and HG-treated H9C2 cells. Data were analyzed by the unpaired t test; **P<0.01. (**F**) Immunofluorescence staining of γH2AX in NG (5.5 mmol/L D-glucose)-treated and HG (35 mmol/L D-glucose)-treated H9C2 cells. Data were analyzed by the unpaired t test; *P<0.05, **P<0.01, ***P<0.001. (**G, H**) Western blot detection of cell cycle-related p53 and p16 protein levels, and the SASP-related proteins MCP1, IL-1α, IL-6, and GDF15 in NG (5.5 mmol/L D-glucose)-treated and HG (35 mmol/L D-glucose)-treated H9C2 cells. β-actin served as an internal reference. Data were analyzed by the unpaired t test, *P<0.05, **P<0.01, ***P<0.001.

Figure 4. Cardiac function and cellular senescence analysis in rats with or without *Rnd3* gene-targeted intervention. (**A**) Schematic diagram of the establishment of T2DM rats. (**B**) Representative images of echocardiography. (**C**) Cardiac function in rats with or without *Rnd3* gene intervention. Data were analyzed by the unpaired t test; *P<0.05, **P<0.01, ***P<0.001. ns, no significance. (**D**) Western blot detection of protein levels of Rnd3, cell cycle-related p53 and p16, and the SASP-related markers MCP1, IL-1α, IL-6, and GDF15 in rats with or without *Rnd3* gene intervention. β-actin served as an internal reference. (**E**) Quantitative analysis of protein levels of Rnd3, cell cycle-related p53 and p16, and the SASP-related factors MCP1, IL-1α, IL-6, and GDF15 in rats with or without *Rnd3* gene intervention. Data were analyzed by the unpaired t test, *P<0.05, **P<0.01, ***P<0.001. ns, no significance. (**F, H**) Immunofluorescence staining of γH2AX in heart tissue of rats with or without *Rnd3* gene intervention. Data were

analyzed by the unpaired t test; Bars = 100 μm. *P<0.05, ***P<0.001. ns, no significance. (**G, I**) SA-β-galactosidase staining in frozen sections of the heart in rats with or without *Rnd3* gene intervention. Data were analyzed by the unpaired t test; Bars = 50 μm. *P<0.05, **P<0.01, ***P<0.001, ns, no significance.

Figure 5. Function and expression of miR-103a-3p. (**A**) Kyoto Encyclopedia of Genes and Genomes (KEGG) analysis of miR-103a-3p. KEGG items in the red box indicate that miR-103a-3p is related to cellular senescence and diabetes. (**B**) Quantitative RT-PCR detection of miR-103a-3p in NG (5.5 mmol/L D-glucose, 72 hours)-treated and HG (35 mmol/L D-glucose, 72 hours)-treated cardiomyocytes. Data were analyzed by the unpaired t test; ***P<0.001. (**C**) Analysis of binding sites between miR-103a-3p and the human and rat *Rnd3* gene 3′UTR. (**D**) The dual luciferase reporter gene method was used to detect the binding effect of miR-103a-3p with the rat *Rnd3* gene 3′UTR. Groups 4 and 5 served as negative and positive controls to demonstrate the reliability of the experimental system. Data were analyzed by the Bonferroni post-hoc test post-one-way analysis of variance; ***P<0.001. (**E**) Quantitative RT-PCR detection of miR-103a-3p in serum samples of a clinical cohort of T2DM (n=24) and controls (n=17). Data were analyzed by the Mann–Whitney test; ****P<0.0001. (**F**) Pearson correlation analysis of miR-103a-3p levels with fasting blood glucose (FBG) and the triglyceride and glucose index (Tyg) in a clinical cohort (n=41).

Figure 6. Effects of an miR-103a-3p inhibitor on *Rnd3* expression and cardiomyocyte

senescence. (**A**) Western blot detection of Rnd3 and cell cycle-related p53 and p16 protein levels, and the SASP-related markers MCP1, IL-1α, IL-6, and GDF15 in HG (35 mmol/L)-treated H9C2 cells. β-actin served as an internal reference. (**B**) Quantitative analysis of protein levels of Rnd3, cell cycle-related p53 and p16, and the SASP-related markers MCP1, IL-1α, IL-6, and GDF15 in HG (35 mmol/L)-treated H9C2 cells. Data were analyzed by the unpaired t test; *P<0.05, **P<0.01, ***P<0.001. (**C**) SA-β-galactosidase and γH2AX staining in HG (35 mmol/L)-treated H9C2 cells. Data were analyzed by the unpaired t test; ***P<0.001.

Figure 7. Cardiac function and cellular senescence analysis in rats treated with miR-103a-3p sponges. (**A**) Schematic diagram of the establishment of T2DM rats. (**B**) Representative images of echocardiography. (**C**) Cardiac function in rats with or without miR-103a-3p inhibition. Data were analyzed by the unpaired t test; *P<0.05, **P<0.01. ns, no significance. (**D**) Western blot detection of Rnd3 and cell cycle-related p53 and p16 protein levels, and the SASP-related markers MCP1, IL-1α, IL-6, and GDF15 in rats with or without miR-103a-3p inhibition. β-actin served as an internal reference. Data were analyzed by the unpaired t test; *P<0.05, **P<0.01. ns, no significance. (**E, G**) Immunofluorescence staining and quantitative analysis of γH2AX in heart tissue of rats with or without miR-103a-3p inhibition. Data were analyzed by the unpaired t test; ***P<0.001. ns, no significance. (**F, H**) SA-β-galactosidase staining in frozen sections of the heart in rats with or without miR-103a-3p inhibition. Data were analyzed by the unpaired t test; *P<0.01, ***P<0.001. ns, no significance.

Figure 8. Interaction of Rnd3 with STAT3 in cardiomyocytes and its role in high glucose (HG) -induced cellular senescence. (**A**) Western blot detection of the STAT3 inhibitor S3I-201 and its effect on STAT3 activation and cellular senescence in HG (35 mmol/L D-glucose) -treated H9C2 cells. β-actin served as an internal reference. (**B**) Upregulation of p-STAT3(Tyr705) in H9C2 cells post HG (35 mmol/L D-glucose) stimuli for 48h. Histone 3 served as an internal reference. (**C**) Ubiquitination mediated p-STAT3(Tyr705) degradation in wild and *Rnd3* KO H9C2 cardiomyocytes. (**D**) Interaction of Rnd3 and STAT3 assessed by Co-Immunoprecipitation. (**E**) Immunofluorescence detection of the expression and intracellular localization of p-STAT3(Tyr705) in HG (35 mmol/l D-glucose) stimulated H9C2 cells by STAT3 inhibitor S3I-201. Bars = 100 μm. (**F**) STAT3 inhibitor S3I-201 suppresses HG (35 mmol/l D-glucose) induced H9C2 cardiomyocyte senescence. Bars = 50 μm. *$P<0.05$, **$P<0.01$. (F)Schematic diagram of the mechanism of how diabetes mediates cardiomyocyte senescence. Diabetes upregulates miR103a-3p expression, further inhibiting Rnd3 expression in cardiomyocytes, and then activates STAT3 signaling to induce the SASP phenotype, and finally mediates the senescence of cardiomyocytes. An miR-103a-3p inhibitor, STAT3 inhibitor, and Rnd3-targeted recovery by AAV9 are helpful to treat cardiomyocyte senescence induced by diabetes.

Novelty and Significance

What Is Known?

1. Rnd3 plays an important role in the setting of certain of cardiovascular diseases, including inflammatory responses after myocardial infarction, diabetic myocardial fibers, pressure overload-induced cardiomyocyte apoptosis, angiogenesis after heart failure, and arrhythmia.

2. Knockout of Rnd3 in cardiomyocytes leads to activation of JAK/STAT signaling, and this activation plays a protective or pathogenic role in heart disease.

3. Dysregulation of miR-103a-3p contributes to cancer progression, venous thromboembolism, and organic inflammation, fibrosis, and injury.

What New Information Does This Article Contribute?

1. Rnd3 expression in myocardium was repressed by diabetes and aging.

2. Rnd3 deficiency synergistically contributed to diabetes-induced cardiomyocyte senescence, and overexpression of Rnd3 reversed diabetes-induced cardiomyocyte senescence.

3. Diabetes-induced miR-103a-3p directly bound *Rnd3* 3′UTR and thus modulated *Rnd3* expression, which participated in diabetes-induced cardiomyocyte senescence.

4. Rnd3 promote ubiquitination mediated degradation of STAT3. Activation of STAT3 was involved in *Rnd3* knockout enhancing diabetes-induced cardiomyocyte senescence.

Our findings suggest that diabetes upregulates miR-103a-3p to inhibit Rnd3 expression, thereby promoting cardiomyocyte senescence, DNA damage, and cardiac dysfunction, and this is mediated by activation of the STAT3 pathway. Targeted inhibition of miR-103a-3p and upregulation of *Rnd3* expression can alleviate the pathological phenotype of diabetes-induced cardiomyocyte senescence, thereby delaying the progression of

diabetic cardiomyopathy.

Nonstandard Abbreviations and Acronyms

DCM Diabetes cardiomyopathy

cTnI Cardiac troponin I

E/A Ratio of E/A

GDF-15 Growth differentiation factor 15

HG High glucose

IL1a Interleukin-1α

IL6 Interleukin-6

MCP-1 Monocyte chemoattractant protein-1

NG Normal glucose

SASP Senescence-associated secretory phenotype

STAT3 Signal transducer and activator of transcription 3

STZ Streptozocin

T1DM Type 1 diabetes mellitus

T2DM Type 2 diabetes mellitus

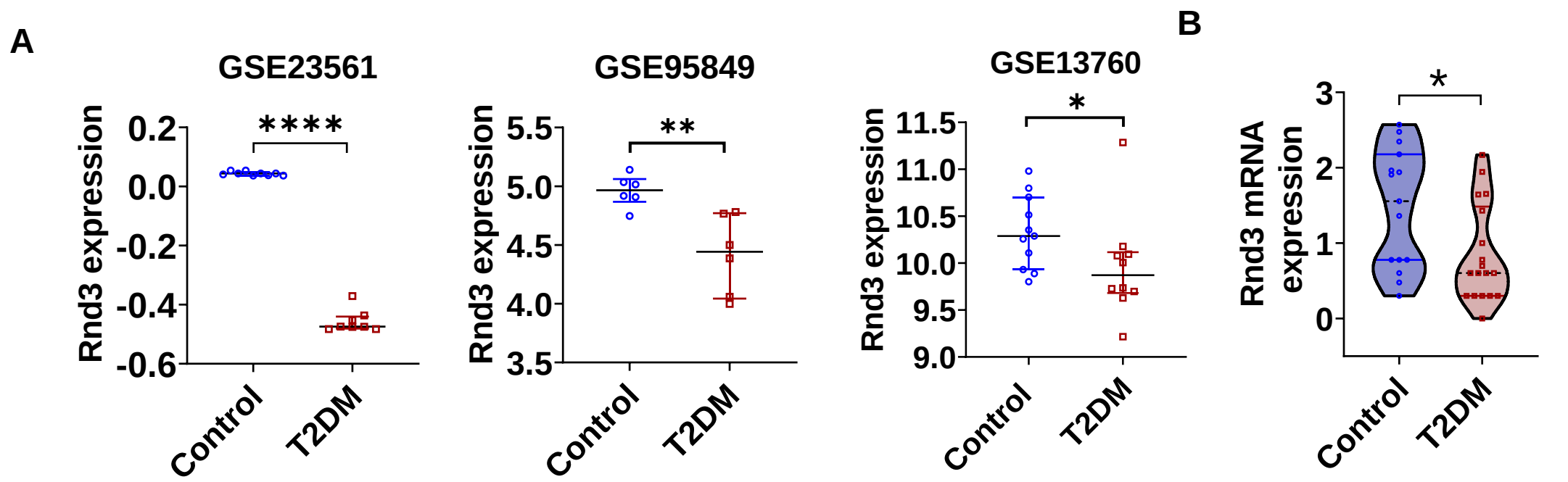

C

	Rnd3	FBG	Age	CTnI	Myoglobin	NT-proBNP	EF%	E/A
Rnd3	1.00	-0.39	-0.55	-0.47	-0.64	-0.41	0.56	0.43
FBG	-0.39	1.00	0.14	0.28	0.36	0.38	-0.33	-0.21
Age	-0.55	0.14	1.00	0.18	0.28	0.36	-0.19	-0.25
CTnI	-0.47	0.28	0.18	1.00	0.56	0.26	-0.24	-0.05
Myoglobin	-0.64	0.36	0.28	0.56	1.00	0.43	-0.34	-0.35
NT-proBNP	-0.41	0.38	0.36	0.26	0.43	1.00	-0.28	-0.46
EF%	0.56	-0.33	-0.19	-0.24	-0.34	-0.28	1.00	0.49
E/A	0.43	-0.21	-0.25	-0.05	-0.35	-0.46	0.49	1.00

1.0
0.5
0
-0.5
-1.0

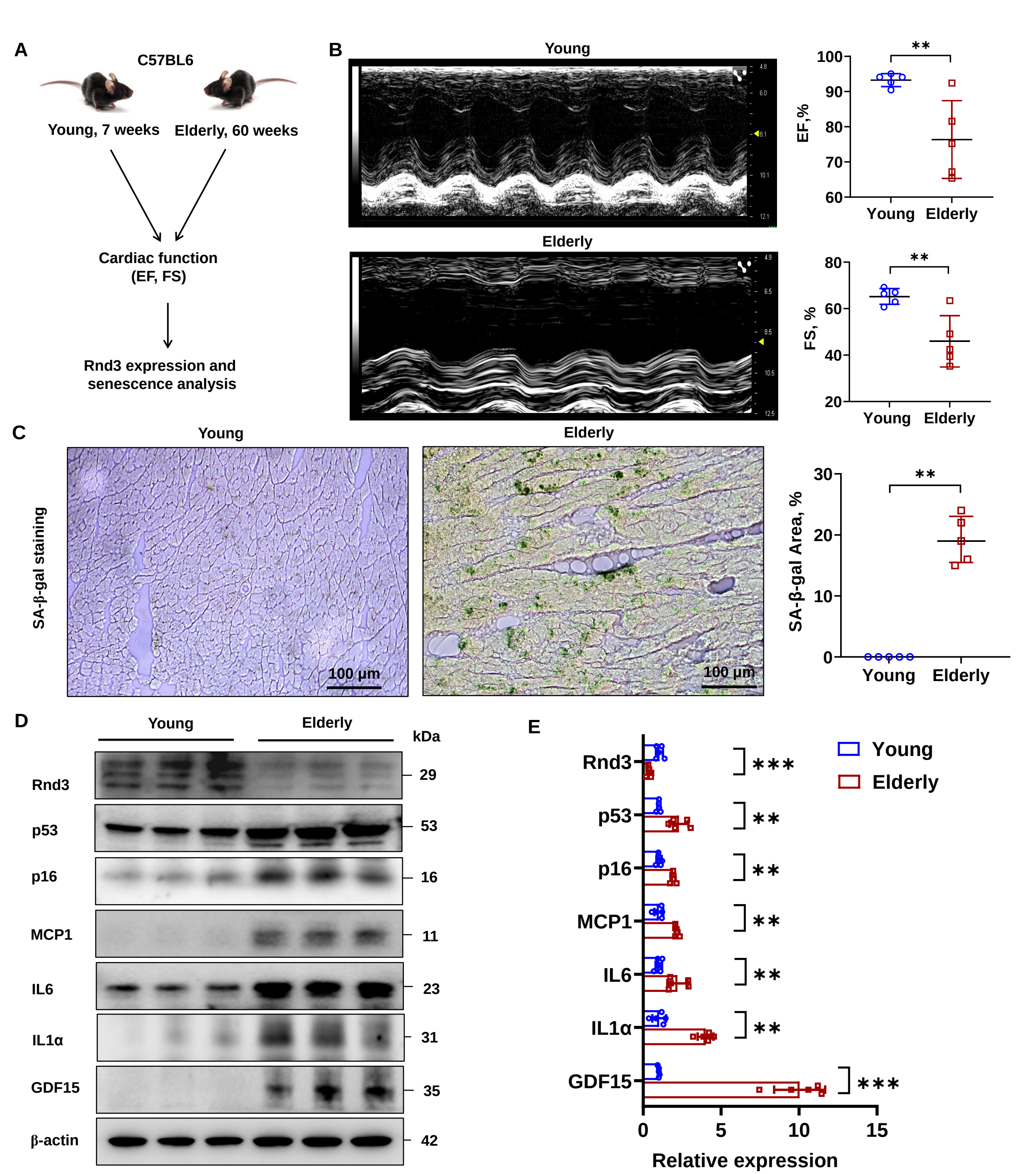
A
C57BL6
Young, 7 weeks
Elderly, 60 weeks
Cardiac function
(EF, FS)
Rnd3 expression and
senescence analysis
B
Young
Elderly
EF,%
FS, %
Young
Elderly
C
Young
Elderly
SA-β-gal staining
100 μm
100 μm
SA-β-gal Area, %
Young
Elderly
D
Young
Elderly
kDa
Rnd3
p53
p16
MCP1
IL6
IL1α
GDF15
β-actin
29
53
16
11
23
31
35
42
E
Young
Elderly
Rnd3
p53
p16
MCP1
IL6
IL1α
GDF15
Relative expression

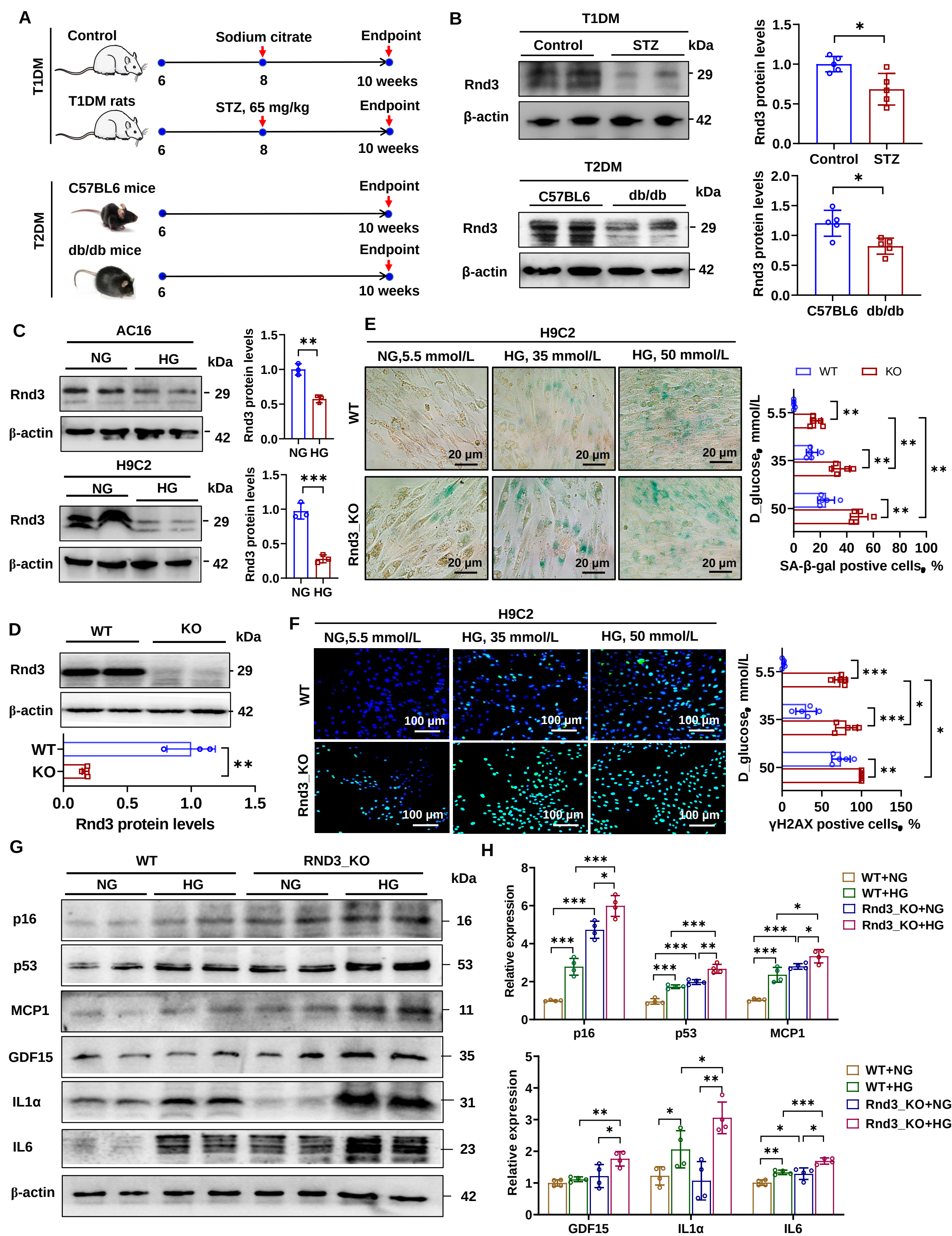
A
T1DM
Control
Sodium citrate
Endpoint
6
8
10 weeks
T1DM rats
STZ, 65 mg/kg
Endpoint
6
8
10 weeks
T2DM
C57BL6 mice
Endpoint
6
10 weeks
db/db mice
Endpoint
6
10 weeks
B
T1DM
Control
STZ
kDa
Rnd3
β-actin
29
42
Rnd3 protein levels
Control
STZ
T2DM
C57BL6
db/db
kDa
Rnd3
β-actin
29
42
Rnd3 protein levels
C57BL6
db/db
C
AC16
NG
HG
kDa
Rnd3
β-actin
29
42
Rnd3 protein levels
NG
HG
H9C2
NG
HG
kDa
Rnd3
β-actin
29
42
Rnd3 protein levels
NG
HG
E
H9C2
NG,5.5 mmol/L
HG, 35 mmol/L
HG, 50 mmol/L
WT
Rnd3_KO
20 μm
WT
KO
D_glucose, mmol/L
SA-β-gal postive cells, %
D
WT
KO
kDa
Rnd3
β-actin
29
42
WT
KO
Rnd3 protein levels
F
H9C2
NG,5.5 mmol/L
HG, 35 mmol/L
HG, 50 mmol/L
WT
Rnd3_KO
100 μm
D_glucose, mmol/L
γH2AX postive cells, %
G
WT
RND3_KO
NG
HG
NG
HG
kDa
p16
p53
MCP1
GDF15
IL1α
IL6
β-actin
16
53
11
35
31
23
42
H
Relative expression
p16
p53
MCP1
WT+NG
WT+HG
Rnd3_KO+NG
Rnd3_KO+HG
Relative expression
GDF15
IL1α
IL6
WT+NG
WT+HG
Rnd3_KO+NG
Rnd3_KO+HG

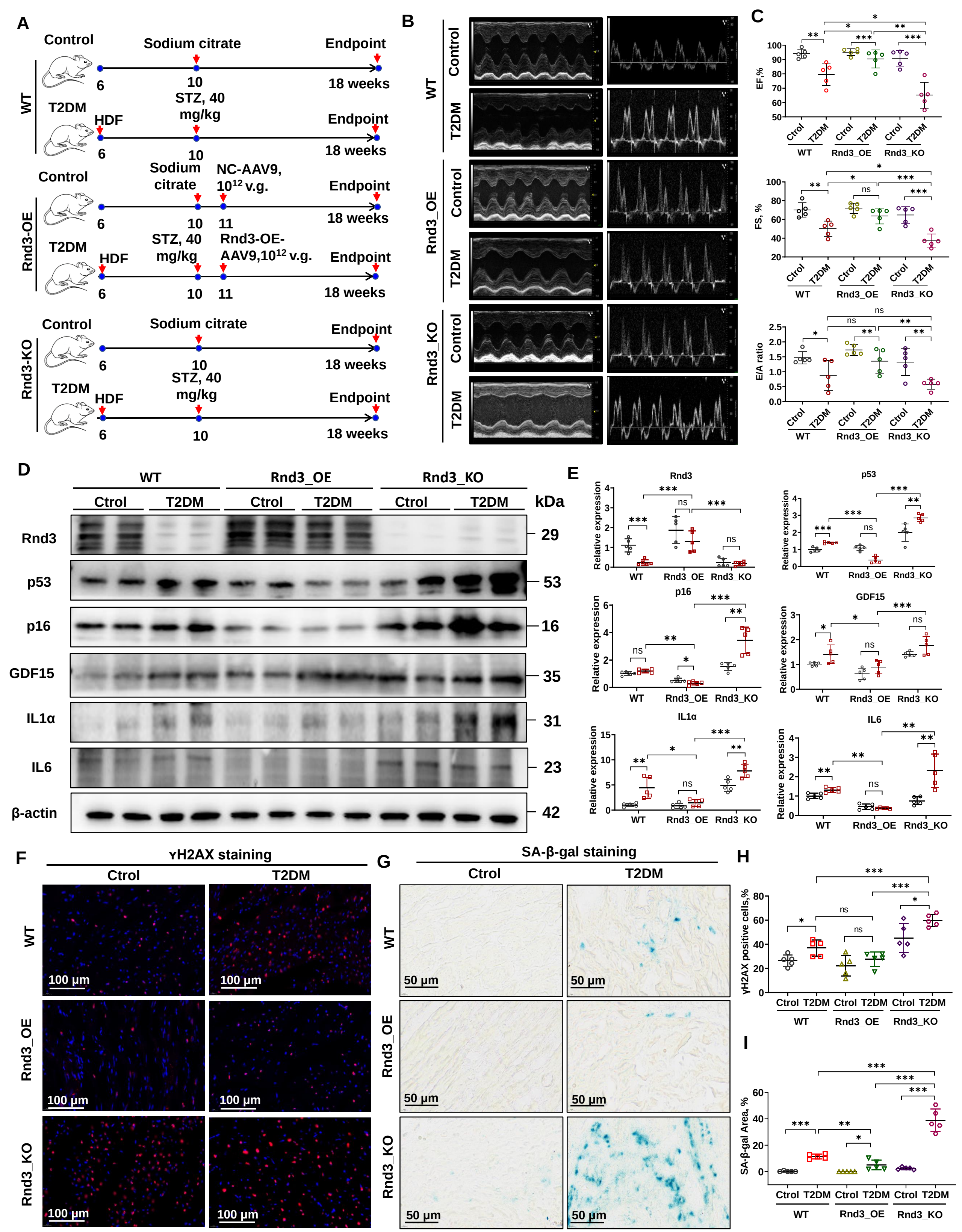
A
Control
Sodium citrate
Endpoint
WT
6
10
18 weeks
T2DM
HDF
STZ, 40 mg/kg
Endpoint
6
10
18 weeks
Control
Sodium citrate
NC-AAV9, 10^12 v.g.
Endpoint
Rnd3-OE
6
10
11
18 weeks
T2DM
HDF
STZ, 40 mg/kg
Rnd3-OE-AAV9,10^12 v.g.
Endpoint
6
10
11
18 weeks
Control
Sodium citrate
Endpoint
Rnd3-KO
6
10
18 weeks
T2DM
HDF
STZ, 40 mg/kg
Endpoint
6
10
18 weeks
B
WT
Control
T2DM
Rnd3_OE
Control
T2DM
Rnd3_KO
Control
T2DM
C
EF,%
FS, %
E/A ratio
Ctrol
T2DM
WT
Rnd3_OE
Rnd3_KO
D
WT
Rnd3_OE
Rnd3_KO
Ctrol
T2DM
kDa
Rnd3
p53
p16
GDF15
IL1α
IL6
β-actin
29
53
16
35
31
23
42
E
Rnd3
p53
p16
GDF15
IL1α
IL6
Relative expression
WT
Rnd3_OE
Rnd3_KO
F
γH2AX staining
Ctrol
T2DM
WT
Rnd3_OE
Rnd3_KO
100 μm
G
SA-β-gal staining
Ctrol
T2DM
WT
Rnd3_OE
Rnd3_KO
50 μm
H
γH2AX positive cells,%
I
SA-β-gal Area, %

A

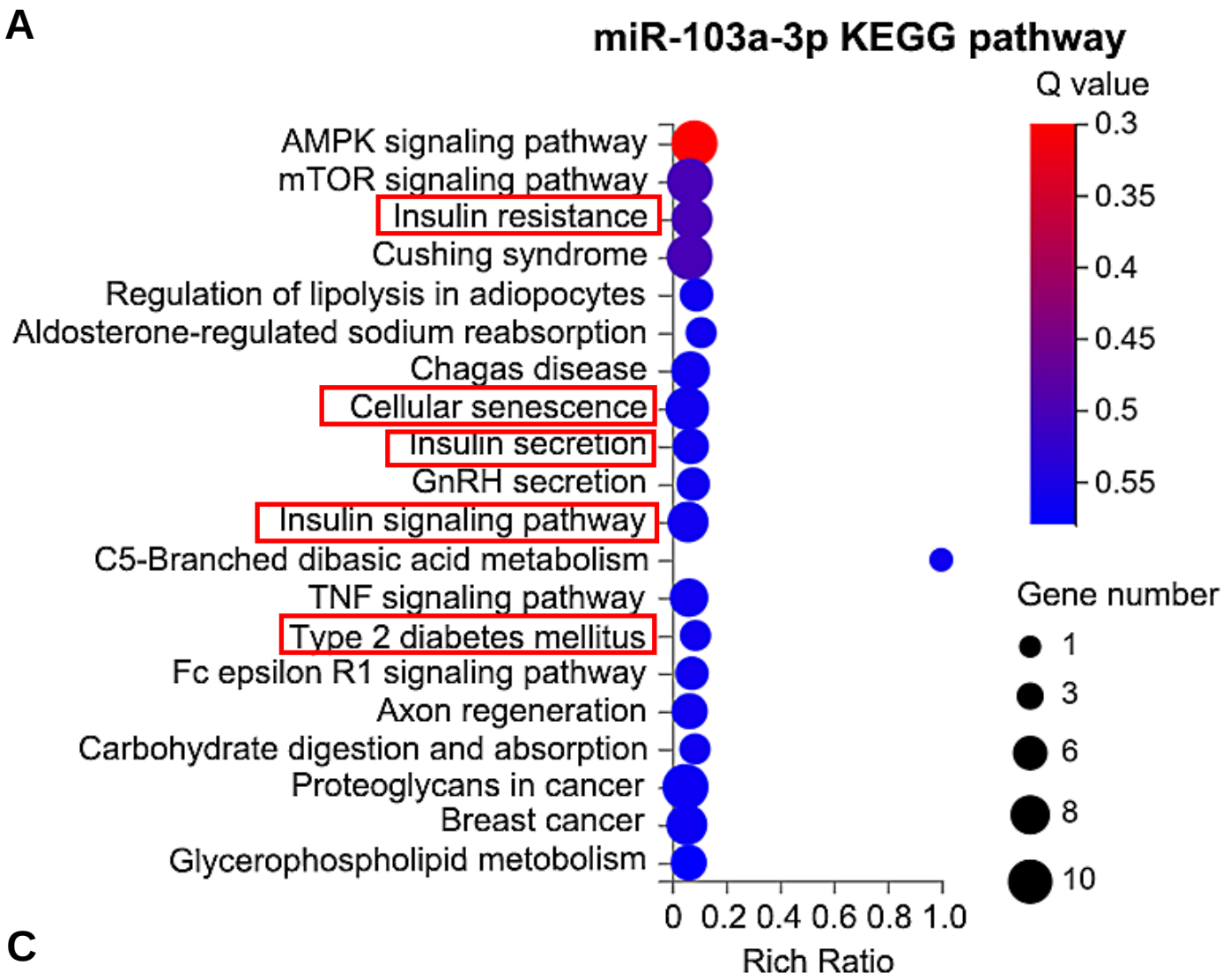

B

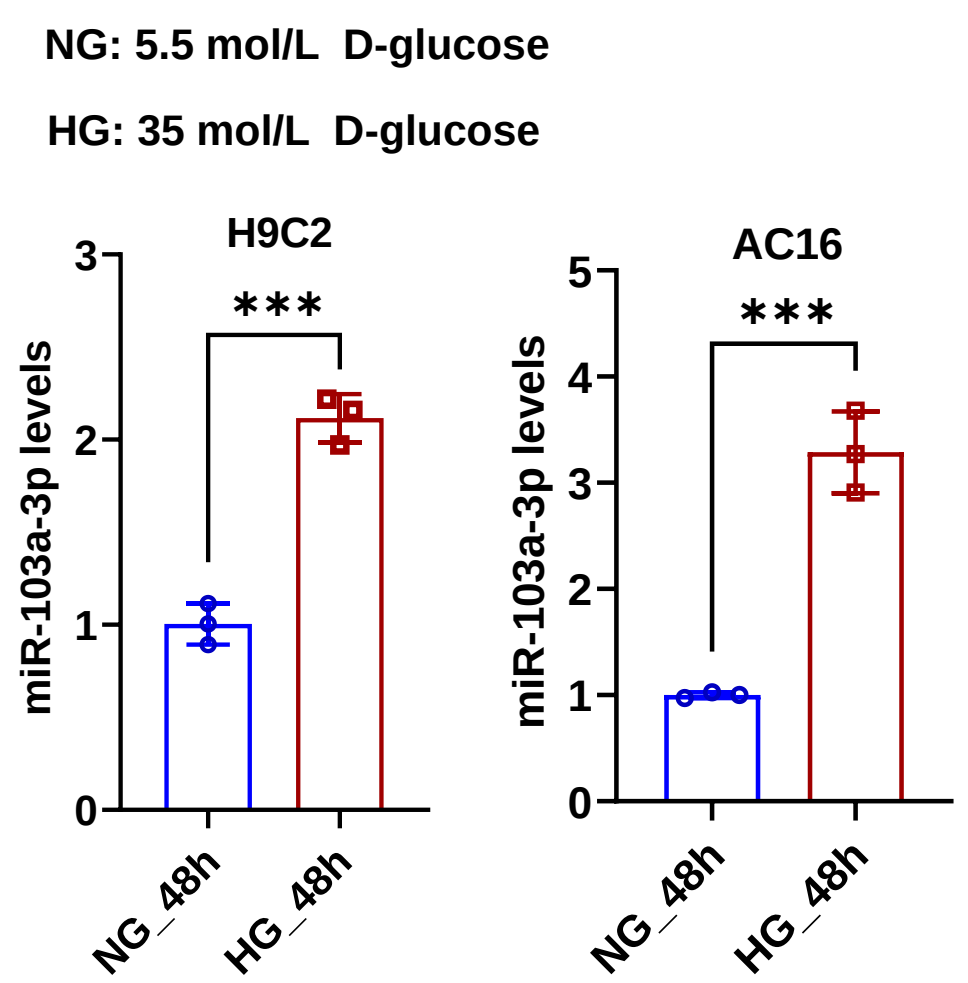

C

Human, *Rnd3* 3'UTR position: 1379

Target 5' G G UUCGUUUUUGAAG UG G 3'
AUAGU C UGU AA GCUGU
UAUCG G ACA UU CGACG
miRNA 3' AG G UG A A 5'

Rat, *Rnd3* 3'UTR position: 579

Target 5' A A G GGAUU GAGGAAAAACU G 3'
GG CCC GUG CGA UGCUGC
UC GGG CAU GUU ACGACG
miRNA 3' AGUA A A 5'

Rat, *Rnd3* 3'UTR position: 716

Target 5' G AUCAA A AAG G U 3'
CGUAG CU G A AGUGUUACU
GUAUC GG C U UUACGACGA
miRNA 3' A G A A G 5'

D

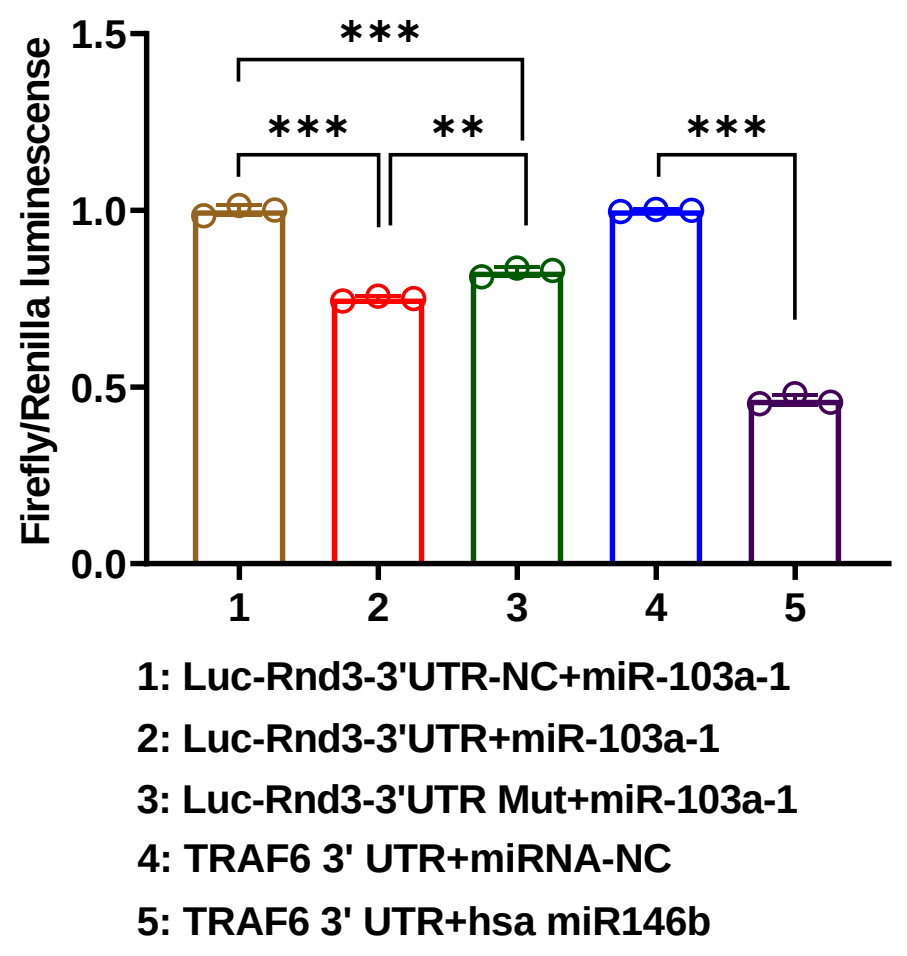

E

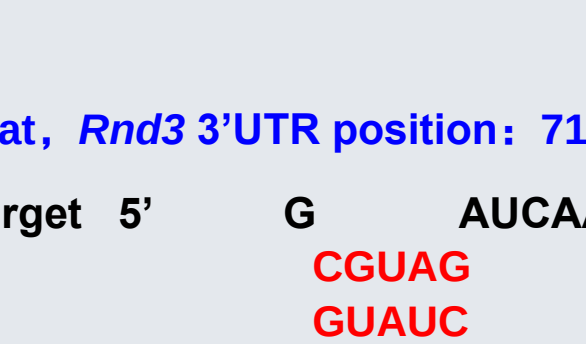

F

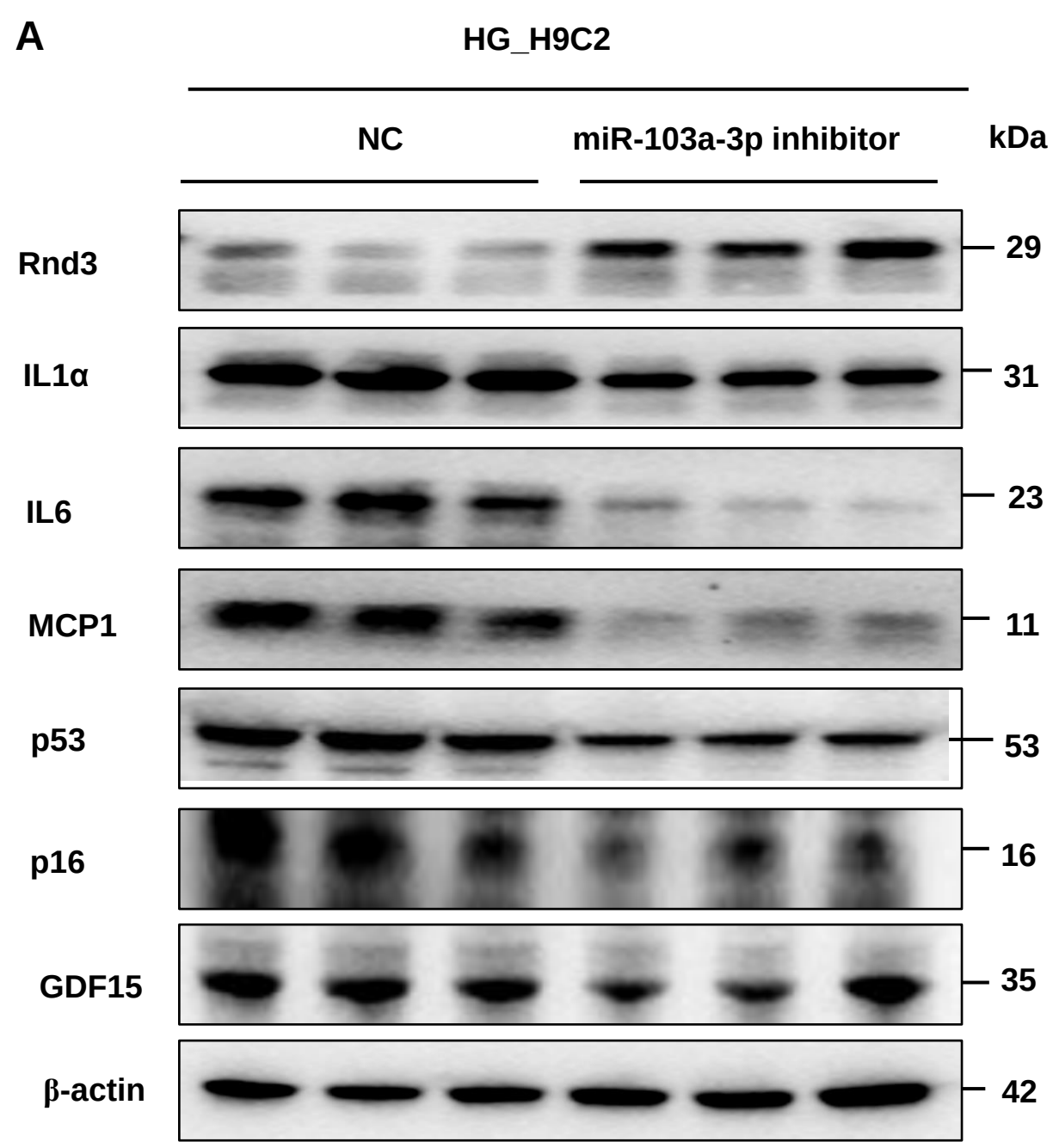
A
HG_H9C2
NC
miR-103a-3p inhibitor
kDa
Rnd3
IL1α
IL6
MCP1
p53
p16
GDF15
β-actin
29
31
23
11
53
16
35
42

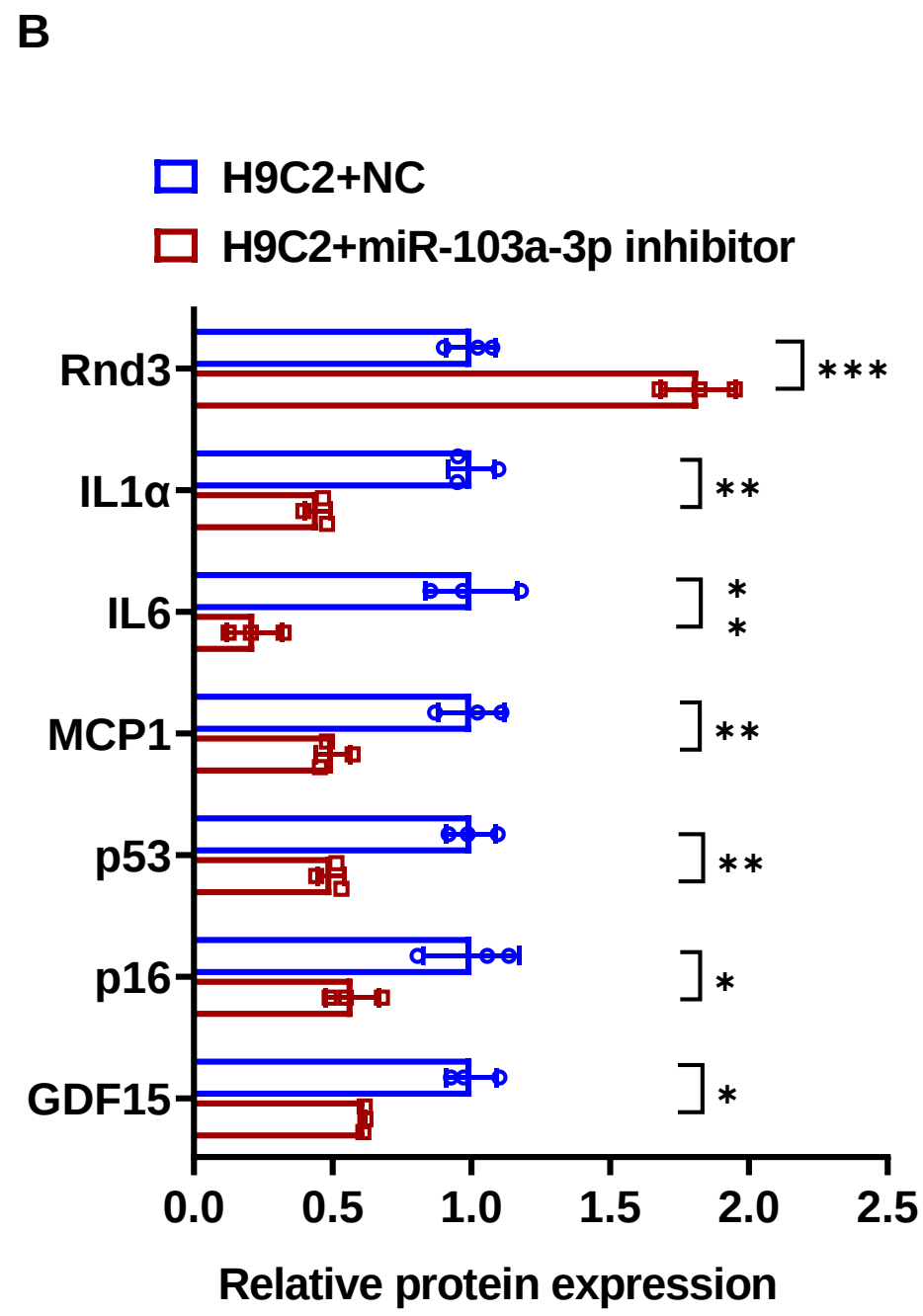
B
H9C2+NC
H9C2+miR-103a-3p inhibitor
Rnd3
IL1α
IL6
MCP1
p53
p16
GDF15
***
**
*
*
**
**
*
*
0.0
0.5
1.0
1.5
2.0
2.5
Relative protein expression

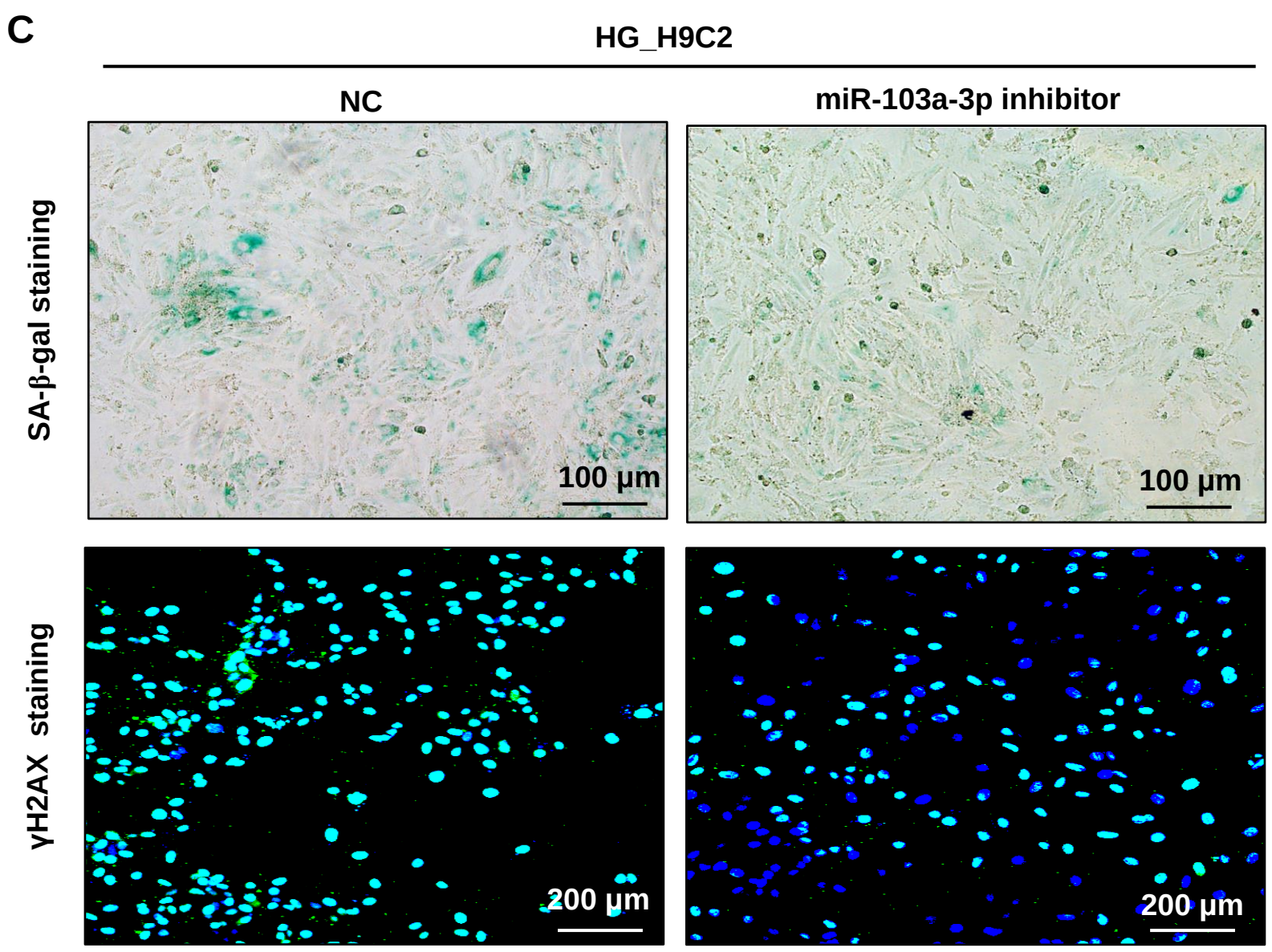
C
HG_H9C2
NC
miR-103a-3p inhibitor
SA-β-gal staining
γH2AX staining
100 μm
100 μm
200 μm
200 μm

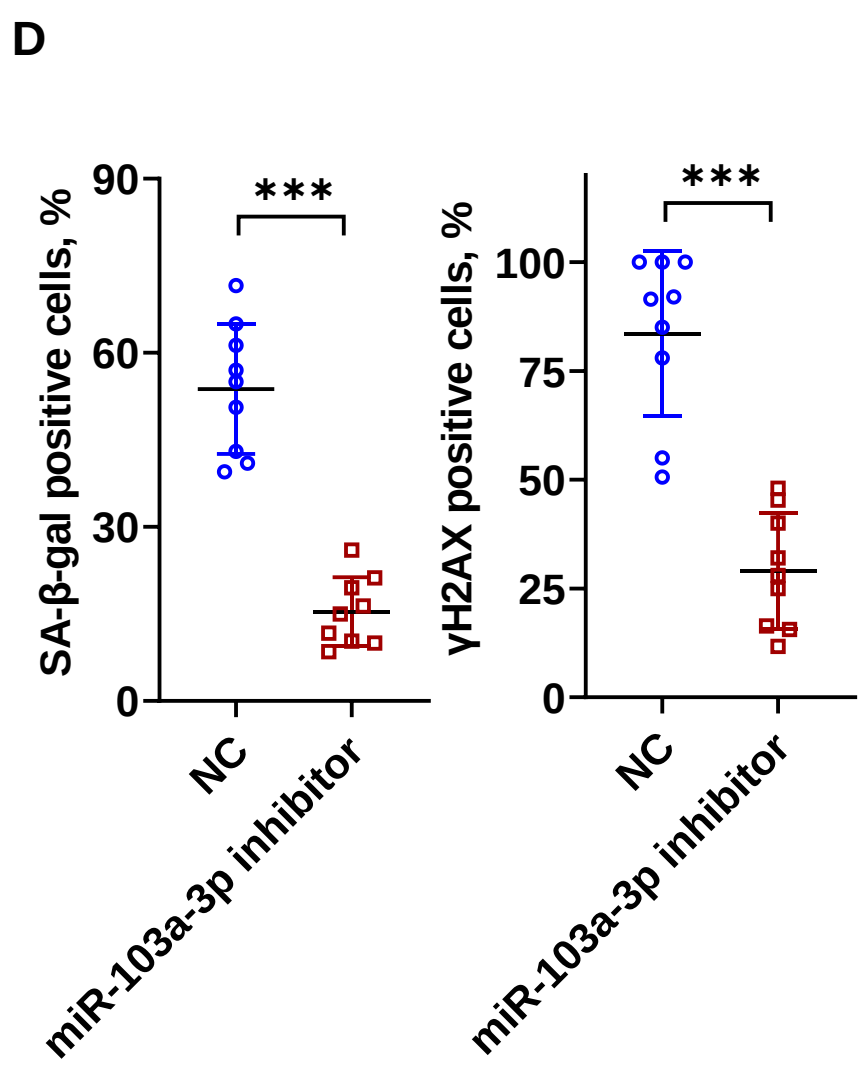
D
SA-β-gal positive cells, %
90
60
30
0
***
NC
miR-103a-3p inhibitor
γH2AX positive cells, %
100
75
50
25
0
***
NC
miR-103a-3p inhibitor

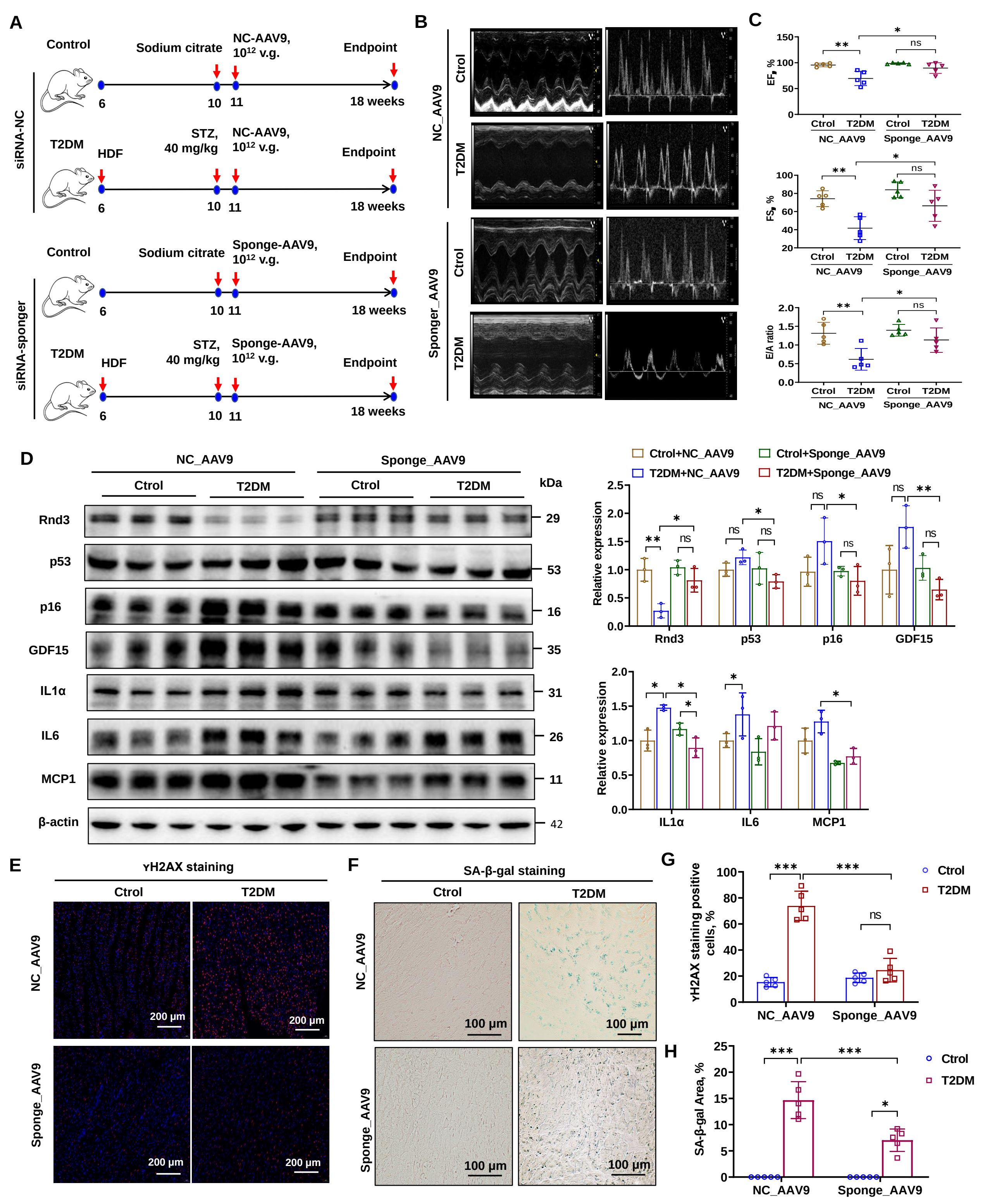
A
siRNA-NC
Control
Sodium citrate
NC-AAV9, 10^12 v.g.
Endpoint
6
10
11
18 weeks
T2DM
HDF
STZ, 40 mg/kg
NC-AAV9, 10^12 v.g.
Endpoint
6
10
11
18 weeks
siRNA-sponger
Control
Sodium citrate
Sponge-AAV9, 10^12 v.g.
Endpoint
6
10
11
18 weeks
T2DM
HDF
STZ, 40 mg/kg
Sponge-AAV9, 10^12 v.g.
Endpoint
6
10
11
18 weeks
B
NC_AAV9
Ctrol
T2DM
Sponger_AAV9
Ctrol
T2DM
C
EF, %
FS, %
E/A ratio
Ctrol
T2DM
NC_AAV9
Sponge_AAV9
D
NC_AAV9
Sponge_AAV9
Ctrol
T2DM
kDa
Rnd3
p53
p16
GDF15
IL1α
IL6
MCP1
β-actin
29
53
16
35
31
26
11
42
Ctrol+NC_AAV9
Ctrol+Sponge_AAV9
T2DM+NC_AAV9
T2DM+Sponge_AAV9
Relative expression
Rnd3
p53
p16
GDF15
IL1α
IL6
MCP1
E
γH2AX staining
Ctrol
T2DM
NC_AAV9
Sponge_AAV9
200 μm
F
SA-β-gal staining
Ctrol
T2DM
NC_AAV9
Sponge_AAV9
100 μm
G
γH2AX staining positive cells, %
Ctrol
T2DM
NC_AAV9
Sponge_AAV9
H
SA-β-gal Area, %
Ctrol
T2DM
NC_AAV9
Sponge_AAV9

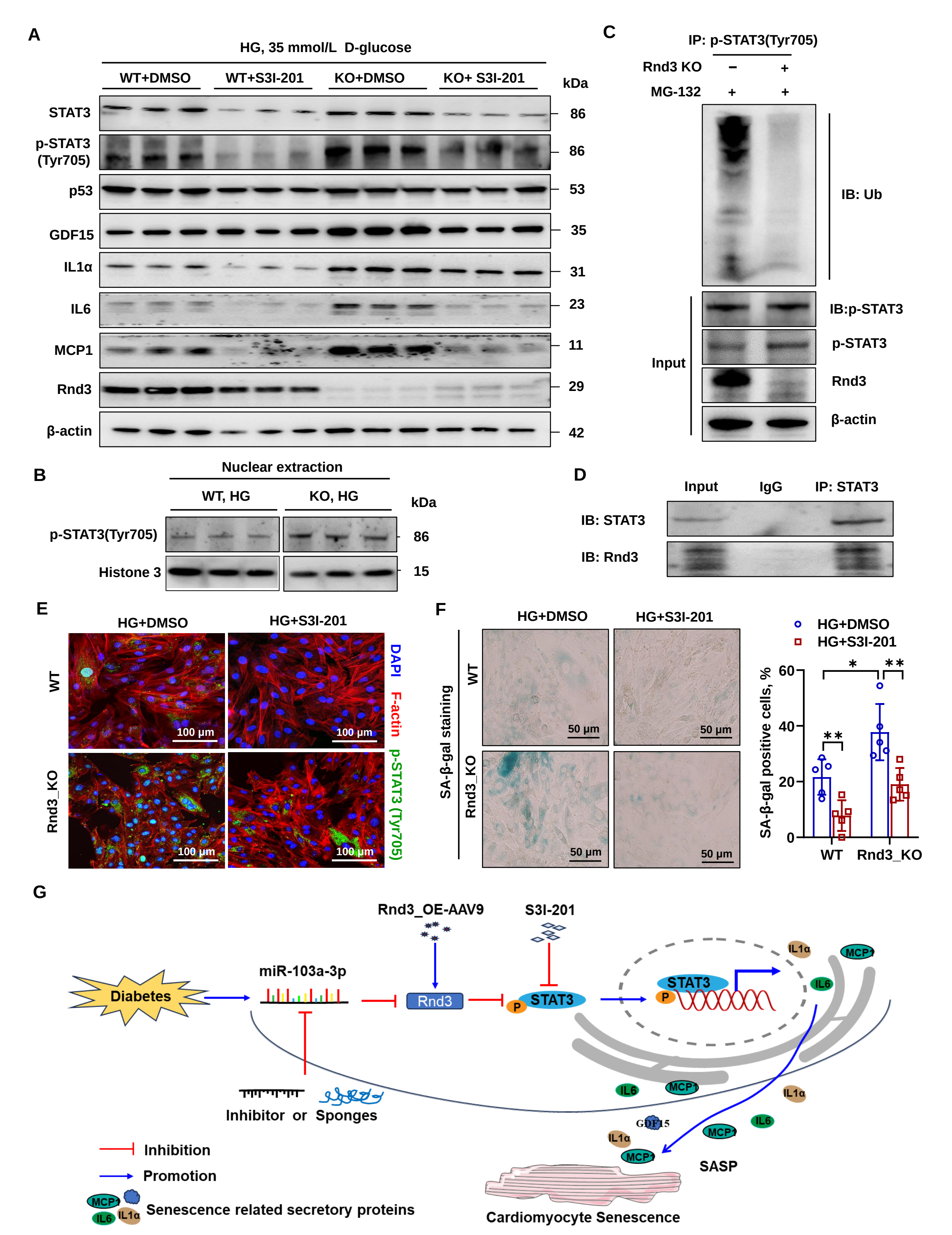
A
HG, 35 mmol/L D-glucose
WT+DMSO
WT+S3I-201
KO+DMSO
KO+ S3I-201
kDa
STAT3
p-STAT3 (Tyr705)
p53
GDF15
IL1α
IL6
MCP1
Rnd3
β-actin
86
86
53
35
31
23
11
29
42
B
Nuclear extraction
WT, HG
KO, HG
kDa
p-STAT3(Tyr705)
Histone 3
86
15
C
IP: p-STAT3(Tyr705)
Rnd3 KO
MG-132
IB: Ub
Input
IB:p-STAT3
p-STAT3
Rnd3
β-actin
D
Input
IgG
IP: STAT3
IB: STAT3
IB: Rnd3
E
HG+DMSO
HG+S3I-201
WT
Rnd3_KO
DAPI
F-actin
p-STAT3 (Tyr705)
100 μm
F
HG+DMSO
HG+S3I-201
SA-β-gal staining
WT
Rnd3_KO
50 μm
HG+DMSO
HG+S3I-201
SA-β-gal positive cells, %
60
40
20
0
*
**
**
WT
Rnd3_KO
G
Rnd3_OE-AAV9
S3I-201
Diabetes
miR-103a-3p
Rnd3
P
STAT3
STAT3
P
IL1α
MCP1
IL6
Inhibitor or Sponges
GDF15
SASP
Cardiomyocyte Senescence
Inhibition
Promotion
Senescence related secretory proteins